APPLICATIONS OF HYPERGRAPHIC MATRIX MINORS VIA CONTRIBUTORS

by

Josephine Elizabeth Anne Reynes, B.S.

A thesis submitted to the Graduate Council of
Texas State University in partial fulfillment
of the requirement for the degree of
Master of Science
with a Major in Mathematics
May 2021

Committee Members:

Lucas Rusnak, Chair

Eugene Curtin

Jian Shen

FAIR USE AND AUTHOR'S PERMISSION STATEMENT

DEDICATION

To my grandfather, the big bad wolf.

Elsie Piddock loved skipping rope so much she could do it forever.

Mathematics is my forever love.

I hope you would be proud.

ACKNOWLEDGEMENTS

I would like to begin by thanking my advisor, Dr. Lucas Rusnak. It has been a joy to work with you, and I have learned so much from this experience. You went above and beyond what you had to do: from encouraging me to present and helping me prepare to helping me select and apply for Ph.D. programs. As I go on to my Ph.D. program and continue my research, I will continue to use all the things you have taught me. The opportunities I've had and future I see ahead may never have happened without your help, and I will be forever grateful for all that you have done for me.

To my thesis committee, Dr. Shen and Dr. Curtin, thank you so much, for the time you have put into reading this work. Dr. Shen, I enjoyed taking your combinatorics class so much and the Discrete Math seminar has been amazing every time I have attended. Dr. Curtin, the first time I ever taught a lab it was for your Calc I class. You gave me freedom to run the lab myself, and this experience helped me realize I wanted to become a professor. I also had a really great time taking graduate level topology with you. Thank you both so much. I would also like to thank the rest of the Department of Mathematics. You were all so welcoming, encouraging, and knowledgeable. I could not imagine a better department to have done my Master's degree in. I would especially like to thank Problem Solvers. Since the very first meeting I attended, I knew this group was something special. I would also like to thank MathWorks. Specifically, Skyler Johnson and Peter Ye, who helped with the Kirchhoff work, and Russell Li, Eric Yan, and Justin Yu, who helped with the Hadamard research.

I would also like to thank my mother, Mary, and my grandmother, Madère. You have both always encouraged me and believed that this was something I was capable of doing. Mom, I hope that if I am ever a parent I do just as an amazing job as you did. Grandma, you listened to me talk, even when it probably made no sense to you. I'm so lucky that of all the mothers and grandmothers in the world, you are the people I get to have as mine. To all of my family, of all the people I could be related to, I'm glad it is you, and I cannot wait to see you again.

Finally, to my roommate, Maria, and friend, Elise. To Maria, Covid-19 has been crazy, and I am so lucky to have been fortunate enough to spend it with a friend. I will be able to fondly remember the pickling, baking, camping, and arts and crafts we did. Thank you for sharing this part of the journey with me. To Elise, you have been here for this entire experience. Even though math is not your department, you helped me edit this thesis, and I am so grateful to have you as a friend. To you both, when I look back on this time in my life, I will choose to remember the fun we had and be filled with joy.

TABLE OF CONTENTS

LIST OF FIGURES

ABSTRACT

Hypergraphic matrix-minors via contributors can be utilized in a variety of ways. Specifically, this thesis illustrates that they are useful in extending Kirchhoff-type Laws to signed graphs and to reinterpret Hadamard's maximum determinant problem.

First, we discuss how the incidence-oriented structures of bidirected graphs allow for a generalization of transpedances which enables the extension of Kirchhoff-type laws to signed graphs. Reduced incidence-based cycle covers, or contributors, form Boolean classes, and the single-element classes are equivalent to Tutte's 2-arborescences. When using entire Boolean classes, which naturally cancel in a graph, a generalized contributor-transpedance is introduced and graph conservation is shown to be a property of the trivial Boolean classes. These contributor-transpedances on signed graphs produce non-conservative Kirchhoff-type Laws based on each contributor having a unique source-sink path. Additionally, the signless Laplacian is used to calculate the maximum value of a contributor-transpedance.

Second, we discuss how hypergraphic matrix-minors via contributors can be used to calculate the determinant of a given $\{\pm 1\}$-matrix. This is done by examining classes of contributors that have multiple symmetries. The oriented hypergraphic Laplacian and the incidence-based notion of cycle-covers allow for this analysis. If a family of these cycle-covers is non-edge-monic, it will sum to zero in every determinant which means the only remaining, $n!$ edge-monic families are counted. Also, any one of them can be utilized to determine the absolute value of the determinant. Hadamard's maximum determinant problem is equivalent to

optimizing the number of locally signed circles of a specified sign in an edge-monic families or across all edge-monic families. Theta-subgraphs have different fundamental circles that yield various symmetries regarding the orthogonality condition, which are equivalent to $\{0, +1\}$-matrices.

1 INTRODUCTION

Graphs and integer matrices are interlocked. This relationship allows for a wide variety of techniques to study both matrix and graph theory problems. Using incidence structures we can translate between matrices and hypergraphs. An incidence matrix of a hypergraph with vertex set V and edge set E is a $V \times E$ matrix where each (v, e)-entry is associated to an incidence. Given any incidence matrix H, the Laplacian is HH^T, and it contains both the degree and adjacency information for a hypergraph. The determinant and minors of the Laplacian also provide information about the structure of the hypergraph. Matrix minors are determined by specific coverings of the hypergraph by locally graphic cycle families, called contributors, that are a refinement of permutations to express minors via a finest possible sum of natural subobjects.

A signed graph is a generalization of a graph where each edge receives a sign +1 or −1. These graphs can be used to examine social balance [15]. We also consider incidence-orientations of signed graphs [24], or bidirected graphs. These first appeared in relation to integer programming [10]. This incidence-theoretic approach has led to the incidence-oriented hypergraphic characterization of the Laplacian [6, 17, 20]. These are then generalized to the signed graphic All Minors Matrix-tree Theorem by [5] as well as the signed graphic Sachs' Theorem by [2], and finally to the Total Minor Polynomial by [12].

This thesis will examine problems through matricial, graphic, and hypergraphic structures. First, we consider the graph theoretic problem of extending Kirchhoff-type laws to non-conservative signed graphic analogs. Second, we will consider Hadamard's maximum determinant problem and reinterpret it via hypergraphic families of contributors. These Kirchhoff-type laws utilize contributors to redefine and calculate transpedance values. We also examine source-sink pathings and contributor sorting. The classic Kichhoff's Laws of conservation are natural contributor cancellation of the graphic case. Similar techniques are used to examine Hadamard's maximum determinant conjecture. First, we expand the problem to an n-full oriented hypergraph before reducing the problem to one of the $n!$ edge-monic contributor families where cancellation is minimized. Additionally, we examine the relationships between contributor families.

Kirchhoff-type Laws for signed graphs were done using transpedances by [4]. Non-conservative Kirchhoff-type Laws for directed graphs appear in [22]. We use contributors to generalize this concept of transpedances. A transpedance is a difference in two arborescence counts and is equivalent to determine an ordered second minor of the Laplacian. These are represented as specific degree-2 coefficients of the total minor polynomial that are calculated using contributors. These transpedances are used to label edges to build a combinatorial interpretation of Kirchhoff's Laws. This is accomplished by using the incidence-theoretic approach introduced in [17] to study hypergraphic Laplacians. As well as the incidence-path mapping families, called *contributors*, from [6] that generalize cycle covers and allow us to classify various hypergraphic characteristic polynomials similar to Sachs' Theorem [2, 9]. It was shown in [20] that if all edges are size 2, these generalized cycle covers form Boolean lattices that generalize the Matrix-tree Theorem. These Boolean families are naturally cancellative when G is a graph. Additionally, the trivial single-element classes correspond to spanning trees and provide a basis for the "conservation" of Kirchhoff's Laws.

Transpedances were initially introduced in [4] as a way to translate the packing and cutting problem of dissecting a rectangle into squares to a networking potential problem. Graph flows capacities were determined to be the tree-number given the Matrix-tree Theorem and a combinatorial version of Kirchhoff's Laws as "spanning tree flows" was obtained from ordered second-co-factors of the Laplacian and edges signed by 2-arborescences. We utilize the methods and ideas of [4] to inform the techniques we use to examine signed graphs. The use of the incidence structure and contributors have allowed us to extend the ideas they originally presented.

Hadamard's maximum determinant problem [14] presents a goal to find the maximum determinant of a matrix $\mathbf{H}$ of size n with entries +1 and −1, and establish a simple upper bound of $|\det(\mathbf{H})| \leq n^{n/2}$. A *Hadamard matrix* is a $\{\pm 1\}$-matrix where the rows are mutually orthogonal and obtains the Hadamard bound. An additional conjecture of Hadamard's is that there is a Hadamard matrix for every positive integer $n \equiv 0 \mod 4$. It is known that Hadamard matrices exist for all $n \equiv 0 \mod 4$ up to 664 [16], as checked by computers. Also, there are some infinite families of known Hadamard matrices, for example there is a Hadamard matrix for all 2^n for $n \geq 2$. There are also bounds for $n \not\equiv 0 \mod 4$ matrices presented in [1, 11, 23]. Given a $\{\pm 1\}$-matrix $\mathbf{H}$, we examine sets of minors that form sets of fundamental circles in the associated oriented hypergraph. However, we cannot simply build a Hadamard matrix from the previously known smaller cases. To see this we can consider a theorem of Cohn.

Theorem 1.0.1 (Cohn, [8]) *Let* $\mathbf{H}$ *be a Hadamard matrix of size* n *having a Hadamard submatrix* $\mathbf{M}$ *of size* $m < n$*, then* $m \leq \dfrac{n}{2}$.

There also exists a larger study on excluded and vanishing minors in [3].

Using the incidence-based notion of cycle-covers of an associated Laplacian from [6] and the oriented hypergraphic connection to Hadamard matrices from [18, 19], we introduce a new method to calculate the determinant of any $\{\pm 1\}$-matrix. This provides a locally signed-graphic interpretation of the maximum determinant problem. We also find signed circle conditions from three different fundamental sets of circles. This leads us to a characterization of $n!$ different classes of fundamental circles that are equivalent to the maximum determinant problem. Finally, these concepts, as well as other symmetries, are shown to be connected via theta configurations.

In Section 2, the definitions, examples, and methodologies for examining graphs are discussed. This section begins with the discussion of various types of graphs, starting with the standard graph structure before moving to discuss bidirected and signed graphs and finally hypergraphs. These various types of graphs are unified through a discussion of the incidence structure that was introduced in [24] and extended to hypergraphs by [7, 17, 21]. This incidence structure allows the extension of many graph theoretic concepts and theorems.

In Section 3, we begin with a discussion of transpedances. Then, we define contributor families for any oriented hypergraphs via tails of path maps in Section 3.2. These classes have the structure of the Boolean lattice equivalence classes in [20]. This allows us to establish a bijection, via the Linking Lemma, between single element Boolean classes and 2-arborescences from [4]. Now, we redefined transpedances in Section 3.2.2 to *D-contributor-transpedances* to include all Boolean classes regardless of size. Kirchhoff's Degeneracy and Energy Reversal conditions immediately apply. The D-contributor-transpedance value is then calculated for an arbitrary edge. This shows that the Boolean classes vanish if they contain a positive circle. Thus, if G is a graph, only trivial contributors, which are also 2-arborescences, remain. Finally, section 3.4 proves that all D-contributor-transpedances possess a unique source-sink path property, and the trivial classes used to label the edges sort spanning trees along their source-sink path. Kirchhoff's Cycle and Vertex Conservation Laws are shown to be a property of the trivial Boolean classes, and conservation on non-cancellative Boolean classes (negative classes) cannot be guaranteed.

In Section 4, we discuss a solution to the maximal contributor-transpedance problems via the signless Laplacian and permanent. This permanent version of Kirchhoff's Laws is a contributor count that is true for all oriented hypergraphs.

In Section 5, we begin by discussing a translation of Hadamard's maximal determinant problem to various fundamental sets of circles in oriented hypergraphs that are related by theta-subgraphs. We then use the oriented hypergraphic cycle-cover approach from [6] to show that non-edge-monic cycle-covers are cancellative for $\{\pm 1\}$ matrices. The remaining cycle-covers belong to one of the $n!$ edge-monic families, and the contributor sum of any one of the edge-monic families is equivalent to the determining the absolute value of the determinant of the $\{\pm 1\}$-matrix. Finally in Section 5.4, we discuss a number of symmetries related to the maximum determinant problem. A set of fundamental circles with the minimum number of adjacencies is identified for each edge-monic family that are linked via cross-theta-subgraphs, and the entries of the original $\{\pm 1\}$-matrix are determined via their circle-signs.

2 BACKGROUND

In this section, we will examine a variety of concepts necessary for the extension of Kirchoff's Laws to signed graphs in Section 3, the work done in Sections 4, and for Hadamard's conjecture in Section 5. We begin by examining graphs and their relevant definitions in Section 2.1. From there we examine, two generalizations of graphs, bidirected and signed graphs in Section 2.1.1 and hypergraphs in Section 2.1.2. We then go on to examine associated matrices in Section 2.2, operations in Section 2.2.1, contributors in Section 2.3, and polynomials in Section 2.4 and Section 2.5.

2.1 Graphs

The definitions in this section provide the basic structure for a graph that is used in establishing the results of this paper. These definitions are based upon the work of [17, 21]. This section will present many standard graph theoretic concepts in terms of the incidence structure.

A *graph* $G = (V, E, I, \varsigma, \omega)$ is a set of vertices V, a set of edges E, and a set of incidences I equipped with two functions $\varsigma : I(G) \to V(G)$ and $\omega : I(G) \to E(G)$, where $|\omega^{-1}(e)| \leq 2$. From the definition of a graph, we consider several properties. The *degree of a vertex* v is $|\varsigma^{-1}(v)|$. The *size of an edge* is $|\omega^{-1}(e)|$. A vertex and edge are *incident* via incidence i if $i \in \varsigma^{-1}(v) \cap \omega^{-1}(e)$.

Path properties of graphs are incredibly important for the analysis of a graph. We define various path properties as follows: A *directed path of length* $n/2$ is a non-repeating sequence

$$\overrightarrow{P}_{n/2} = (a_0, i_1, a_1, i_2, a_2, i_3, a_3, ..., a_{n-1}, i_n, a_n)$$

of vertices, edges and incidences, where $\{a_\ell\}$ is an alternating sequence of vertices and edges, and i_h is an incidence between a_{h-1} and a_h. Let $\overrightarrow{P}_1 = (t, i, e, j, h)$ denote a path of length 1 with a distinguished tail vertex t and head vertex h. The incidences i and j are the *tail-incidence* and *head-incidence*, respectively. A *directed weak walk of* G is the image of an incidence-preserving map of a directed path into G.

Using the above information, we can define many connections between incidence, edges, and vertices in terms of the path properties. That is to say, we can distinguish different types of paths by placing restrictions on their sequences of incidences, edges, and vertices. A *path of* G is a vertex, edge, and incidence-monic directed path of length $n/2$. A *backstep of* G is an embedding of $\overrightarrow{P}_1$ into G that is neither incidence-monic nor vertex-monic. A *loop of* G is an embedding of $\overrightarrow{P}_1$ into G that is incidence-monic but not vertex-monic. A *directed adjacency of* G is an embedding of $\overrightarrow{P}_1$ into G that is incidence-monic. A *circle of* G is an embedding of $\overrightarrow{P}_n$ into G that is incidence-monic and vertex-monic with the exception of the initial vertex $a_0 = a_n$. We call this a circle to minimize confusion between an algebraic cycle and this graph component. Furthermore, backsteps are considered to be separate from circles as they do not complete an adjacency. A *digon* is a circle containing exactly two adjacencies.

Example 2.1.1 *Consider the graph in Figure 1. The three vertices are labeled* v_1, v_2, v_3 *and each is connected to two incidences.*

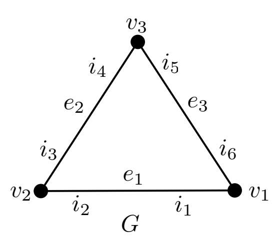

Figure 1: An example of a simple graph.

Thus each vertex has degree 2*. Each edge is connected to two incidences and so the size of each edge is also* 2*. The vertices* v_1 *and* v_2 *are adjacent since the path* $\overrightarrow{P_1} = (v_1, i_1, e_1, i_2, v_2)$ *connects them. The vertices* v_1, v_2, v_3 *form a circle of* G*. For* *simplicity of the figures, incidences may be omitted in future examples; however, all edges and vertices are to be assumed to be bonded by incidences.*

Given a graph, we can also define various components of the graph, and it is these components of graphs that are crucial to the work presented here. A *subgraph* of a graph G is a graph formed by a subset of the original graph's vertex, edge, and incidence sets with a restriction of the original mapping functions. Clearly, a graph must be a subgraph of itself. A *connected component* of G is a subgraph in which a path exists between all pairs of vertices of the subgraph. A graph G is *connected* if G is itself a connected component. A *tree* is a connected acyclic graph. A subgraph H of G is *spanning* if $V(H) = V(G)$, while a *spanning tree* of G is a subgraph of G that is a tree and spanning. The *tree number of* G is the number of spanning trees of G. A *root* of a tree of G is a vertex from which all paths are regarded as emanating from. An k-*arborescence* is a set of k disjoint, rooted trees of G whose union spans G. A 2-*arborescence* of G is a pair of disjoint rooted trees whose union spans G.

Example 2.1.2 *Each subgraph in Figure 2 is acyclic and connected while containing all vertices, and so the subgraphs are all spanning trees of the original graph.*

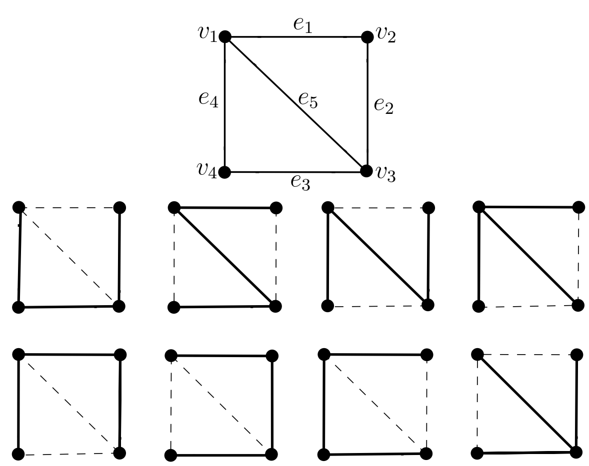

Figure 2: A graph with eight spanning trees.

The original graph, the top graph of the figure, contains four vertices as does each subgraph. Each subgraph also contains a subset of the original graph's incidences and edges.

2.1.1 Bidirected and Signed Graphs

A *bidirected graph* G is a graph equipped with an incidence orientation function $\sigma : I \to \{+1, -1\}$. An incidence with orientation +1 is depicted as an arrow entering a vertex, and an incidence with orientation −1 is depicted as an arrow exiting a vertex. Thus, the *sign of a weak walk* W is

$$sgn(W) = (-1)^{\lfloor n/2 \rfloor} \prod_{h=1}^{n} \sigma(i_h).$$

A *signed graph* is a graph in which each edge is assigned a sign $\{+1, -1\}$ according to the sign of its adjacency.

Example 2.1.3 *Here we can see that all the properties of graphs described in 2.1 still apply to both signed and bidirected graphs. Additionally, we can easily translate between signed and bidirected graphs. An edge with incidences i and j is assigned the sign of $-\sigma(i)\sigma(j)$.*

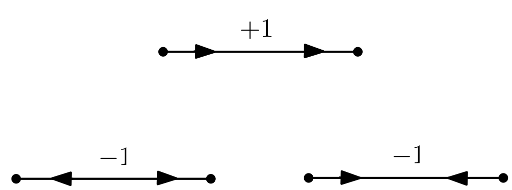

Figure 3: Different orientations of bidirected edges correspond to positively and negatively signed edges in a signed graph.

Now that we have shown the relationship between edge signings and incidence orientations, we will examine how this translates to an entire graph in the next example.

Example 2.1.4 *Translating the edge orientations demonstrated in Figure 3 to the incidences, it can be seen that bidirected graphs are orientations of signed graphs.*

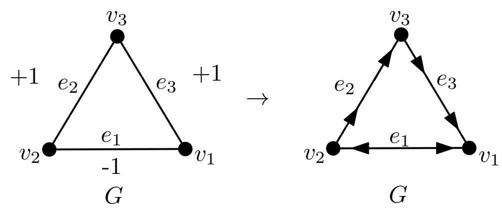

Figure 4: A Signed Graph can be represented as a Bidirected Graph.

2.1.2 Hypergraphs

The previous sections have discussed different types of graphs that do not allow for hyperedges, and so we begin by adapting the definition of a graph first presented in Section 2.1. An *incidence hypergraph* G is a tuple $G = (V, E, I, \varsigma, \omega)$ where V, E and I are disjoint, finite sets of vertices, edges, incidences respectively, $\varsigma : I \to V$, and $\omega : I \to E$. This is the same definition used for graphs with the exception that we have removed the condition requiring $|\omega^{-1}(e)| \leq 2$. The removal of this condition allows edges to be incident to more than two vertices.

Let $G = (V, E, I, \varsigma, \omega)$ be an incidence hypergraph. An *orientation of an incidence hypergraph* G is a signing function $\sigma : I \to \{+1, -1\}$. An *oriented hypergraph* is a sextuple $G = (V, E, I, \varsigma, \omega, \sigma)$ consisting of a set of vertices V, a set of edges E, a set of incidences I, two incidence end maps $\varsigma : I \to V$, and $\omega : I \to E$, and an incidence orientation function $\sigma : I \to \{+1, -1\}$. Incidence orientations of +1 are indicated by an arrow entering a vertex and -1 exiting a vertex.

Given an incidence hypergraph $G = (V, E, I, \varsigma, \omega)$ define the *loading of* G, denoted $L(G)$, as $(V, E, I \cup I_0, \varsigma_L, \omega_L)$ where I_0 is a set of new incidences of the form (v, e) if $\varsigma^{-1}(v) \cap \omega^{-1}(e) = \varnothing$, $\varsigma_L\big|_I = \varsigma$ and $\varsigma_L\big|_{I_0} : (v, e) \mapsto v$, and $\omega_L\big|_I = \omega$ and $\omega_L\big|_{I_0} : (v, e) \mapsto e$. The loading makes any graph a uniform hypergraph as shown in Example 2.1.5. This allows us to talk about incidences that do not exist in the original graph.

Example 2.1.5 *Given the graph in Figure 1, the loading of the graph is shown in Figure 5. The loading of a graph will always be a hypergraph unless the graph is a single vertex or a pair of adjacent vertices.*

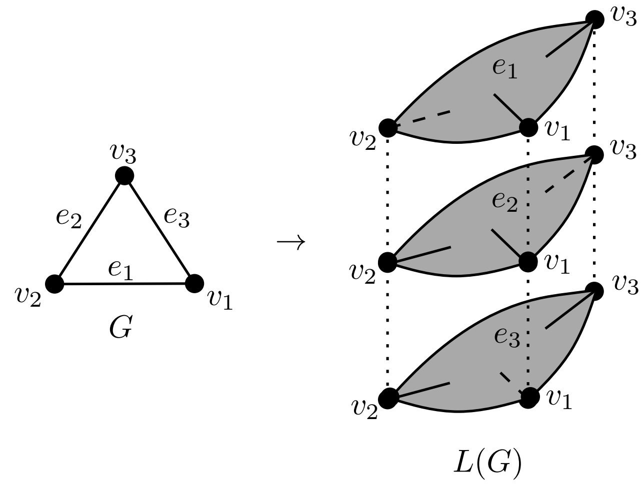

Figure 5: The incidence loading of K_3 to produce a uniform hypergraph.

New incidences appear dashed within each hyperedge, and the vertices are identified along the dashed vertical lines.

A *theta-subgraph* consists of 3 internally-disjoint incidence paths between a and b, where $a, b \in V \cup E$. There are three types of hypergraphic theta-subgraphs that were introduced in [21]; when $a, b \in V$ it is called a *vertex-theta*, when $a, b \in E$ it is called an *edge-theta*, and when a and b consist of a vertex and and edge it is called a *cross-theta*. Cross thetas have been shown in [21] to be the minimal obstruction to balanceability.

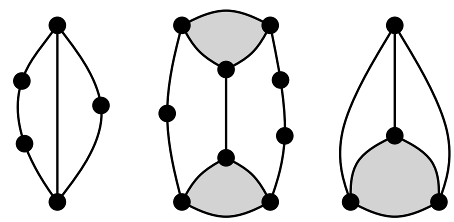

Figure 6: A vertex-, edge-, and cross-theta, respectively.

Lemma 2.1.6 ([21]) *Let Θ be a theta subgraph with circle signs ϵ_1, ϵ_2, and ϵ_3.*

1. *If Θ is a vertex- or edge-theta, then $\epsilon_1 \epsilon_2 = \epsilon_3$.*

2. *If Θ is a cross-theta, then $\epsilon_1 \epsilon_2 = -\epsilon_3$.*

As done with bidirected and signed graphs, we can extend definitions associated with graphs to hypergraphs through the incidence structure.

Example 2.1.7 *In a hypergraph we sign adjacencies locally, instead of signing edges, using the incidence structure. In this example we see that v_1 had degree 1 and v_2 and v_3 both have degree 2. We also see that e_1 has size 3 and edge e_2 has size 2.*

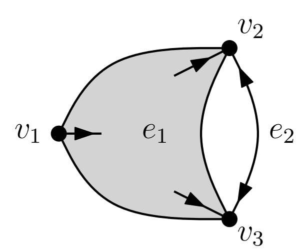

Figure 7: An oriented hypergraph G with oriented incidences

In the oriented hypergraph above we also see the digon between v_2 and v_3 is positive since the adjacencies within the hyperedges and the adjacency on e_2 are both negative. Traveling through e_1 from v_1 to v_2 to v_3 we see that the circle is negative since there is only one negative adjacency in the circle between v_2 and v_3.

2.2 Matrices

Matrices can be used to store information about a graph's structure. This allows for matrix theoretic concepts to be applied to graphs through the examination of four important matrices: the incidence, adjacency, degree, and Laplacian matrix. In Section 2.2.1 and Section 2.4, we will discuss how these matrices are analyzed.

The *incidence matrix* of a graph G is the $V \times E$ matrix $\mathbf{H}_G$ where the (v, e)-entry is the number of incidences $i \in I$ such that $\varsigma(i) = v$ and $\omega(i) = e$. Graphs can be assigned an arbitrary orientation of edges that allows for the signing of incidences.

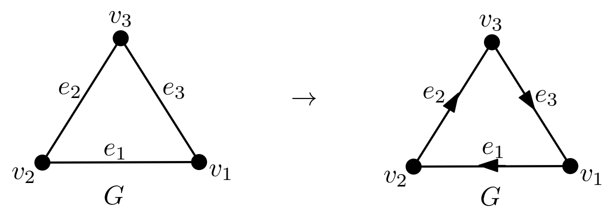

Figure 8: Graph with an orientation assigned to the edges.

The *adjacency matrix* $\mathbf{A}_G$ of a graph G is the $V \times V$ matrix whose (u, w)-entry is the number of adjacencies between vertex u and vertex w. The *degree matrix* of a graph G is the $V \times V$ diagonal matrix whose (v, v)-entry is the number of incidences $i \in I$ such that $\varsigma(i) = v$. The number of incidences at a vertex v is clearly equal to the number of backsteps at v. The *Laplacian matrix of* G is defined as $\mathbf{L}_G := \mathbf{H}_G \mathbf{H}_G^T = \mathbf{D}_G - \mathbf{A}_G$. See [17] for the result that the Laplacian is the 1-weak-walk matrix.

Shown below are the degree, adjacency, incidence, and Laplacian matrix for the graph in Figure 1.

$$\mathbf{D} = \begin{bmatrix} 2 & 0 & 0 \\ 0 & 2 & 0 \\ 0 & 0 & 2 \end{bmatrix}, \quad \mathbf{A} = \begin{bmatrix} 0 & 1 & 1 \\ 1 & 0 & 1 \\ 1 & 1 & 0 \end{bmatrix}, \quad \mathbf{L} = \begin{bmatrix} 2 & -1 & -1 \\ -1 & 2 & -1 \\ -1 & -1 & 2 \end{bmatrix}, \quad \mathbf{H} = \begin{bmatrix} 1 & 0 & -1 \\ -1 & 1 & 0 \\ 0 & -1 & 1 \end{bmatrix}$$

For the Laplacian matrix above, it is clear that the diagonal entries are the degrees and the off diagonal entries are the adjacencies for the graph in Figure 1.

Example 2.2.1 *Consider the oriented hypergraph with its associated incidence matrix* $\mathbf{H}_G$ *and Laplacian matrix* $\mathbf{L}_G$*.*

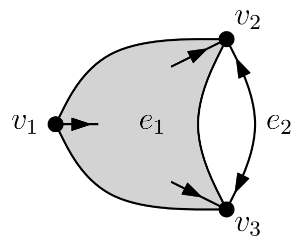

$$\mathbf{H}_G = \begin{bmatrix} -1 & 0 \\ 1 & 1 \\ 1 & 1 \end{bmatrix} \qquad \mathbf{L}_G = \begin{bmatrix} 1 & -1 & -1 \\ -1 & 2 & 2 \\ -1 & 2 & 2 \end{bmatrix}$$

Figure 9: An oriented hypergraph G and its Laplacian.

The signs of the adjacencies can be examined locally. The adjacency from v_2 *to* v_3 *along edge* e_1 *is negative just as the adjacency from* v_2 *to* v_3 *along edge* e_2 *is negative. The sign of the circle, which also happens to be a digon,* $(v_1, e_1, v_2, e_2, v_1)$ *is positive as it is the product of the adjacency signs.*

The $\mathbf{L}_{ij}$ minor of a $n \times n$ matrix is a $(n-1) \times (n-1)$ matrix obtained by removing row i and column j of the original matrix.

2.2.1 Permanents and Determinants

A graph can have its vertex, edge, and incidence sets indexed. This process allows for combinatorial analysis of a graph. A *permutation* π is a bijection from a set S to itself. A *cycle of a permutation* is a cyclic sequence obtained by the compositional closure of π. Every permutation can be written as the product of disjoint cycles; one cycles or fixed points are conventionally omitted.

Example 2.2.2 *If* $S = \{1, 2, 3\}$ *then all possible permutation of* S *are*

$$\{e, (12), (13), (23), (123), (132)\}.$$

The following lemma is well known, and this factorial growth of permutations plays an important role in the complexities of analyzing Hadamard's conjecture through contributors as discussed in Section 5.4.

Lemma 2.2.3 *The total number of permutations of a set with n elements is $n!$.*

Next, we discuss a number of permutation characteristics. An *inversion* in a permutation occurs for every pair (i, j) with $i < j$, where we have $\pi(i) > \pi(j)$. An *even cycle* is a cycle with an odd number of inversions, while an *odd cycle* is a cycle with an even number of inversions. Below we see an example of inversions for the permutation (132).

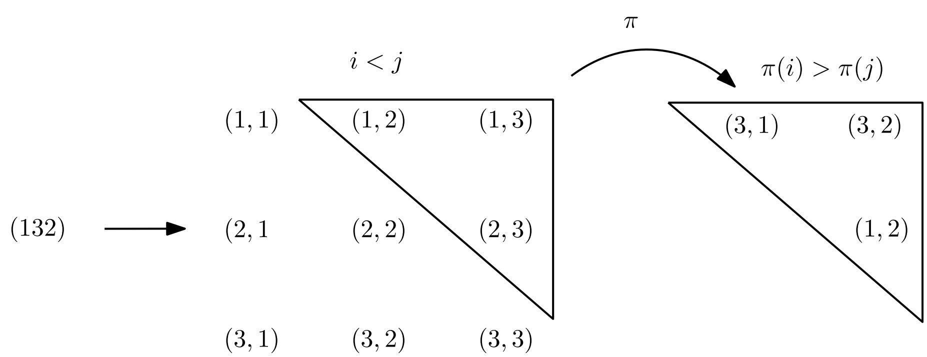

Figure 10: The (i, j) pairs with $i < j$ appear in the triangle. Their image under the permutation $\pi = (132)$ has two inversions, namely, $(3, 1)$ and $(3, 2)$.

Permutations are crucial for the discussion of permanents and determinants given that both are sums over permutations. Given an $n \times n$ matrix $\mathbf{M}$ and S_n a symmetric group of order n, the *permanent* of $\mathbf{M}$ is

$$\operatorname{perm}(\mathbf{M}) = \sum_{\pi \in S_n} \prod_{i \in [n]} m_{i,\pi(i)},$$

and the *determinant* of $\mathbf{M}$ is

$$\det(\mathbf{M}) = \sum_{\pi \in S_n} \epsilon(\pi) \prod_{i \in [n]} m_{i,\pi(i)}.$$

Where $\epsilon(\pi) = (-1)^{inv(\pi)}$, and where $inv(\pi)$ is the number of inversions of π. It is known that $\epsilon(\pi) = (-1)^{ec(\pi)}$ where $ec(\pi)$ is the number of even cycles in π.

Example 2.2.4 *An example of a determinant calculation for the Laplacian of Figure 1 is*

$$
\begin{aligned}
\det\begin{bmatrix} 2 & -1 & -1 \\ -1 & 2 & -1 \\ -1 & -1 & 2 \end{bmatrix} &= (-1)^0 2\begin{bmatrix} 2 & -1 \\ -1 & 2 \end{bmatrix} + (-1)^1(-1)\begin{bmatrix} -1 & -1 \\ -1 & 2 \end{bmatrix} \\
&+ (-1)^2(-1)\begin{bmatrix} -1 & 2 \\ -1 & -1 \end{bmatrix} \\
&= 2[(2\cdot 2) - ((-1)\cdot(-1))] + [(-1)(2) - (-1)(-1)] \\
&- [(-1)(-1) - (-1)(2)] \\
&= 2(4-1) + (-2-1) - (1-(-2)) \\
&= 2(3) + (-3) - (3) \\
&= 0
\end{aligned}
$$

It is a well-known result that the determinant of Laplacian for any graph is zero.

The concepts discussed in this section allow for the concepts discussed in section 2.3 and 2.4.

The *characteristic polynomial of* $\mathbf{M}$ is $\chi_{\mathbf{M}}(x) = det(x\mathbf{I} - \mathbf{M})$ where $\mathbf{I}$ is the identity matrix. In the next example we will see a characteristic polynomial calculation.

Example 2.2.5 *The characteristic polynomial for the matrix in Example 2.2.4.*

$$\det\begin{bmatrix} x-2 & 1 & 1 \\ 1 & x-2 & 1 \\ 1 & 1 & x-2 \end{bmatrix} = (-1)^0(x-2)\begin{bmatrix} x-2 & 1 \\ 1 & x-2 \end{bmatrix} + (-1)^1(1)\begin{bmatrix} 1 & 1 \\ 1 & x-2 \end{bmatrix}$$

$$+ (-1)^2(1)\begin{bmatrix} 1 & x-2 \\ 1 & 1 \end{bmatrix}$$

$$= (x-2)[(x-2)(x-2)-1] + (-1)[(x-2)-1]$$

$$+ (1)[1-(x-2)]$$

$$= (x-2)(x^2-4x+4-1) + (-1)(x-3) + (-x+3)$$

$$= (x^3-4x^2+3x-2x^2+8x-6) + (-x+3) + (-x+3)$$

$$= x^3-6x^2+9x$$

Sachs' Theorem [9] yields a combinatorial count of coefficients of the characteristic polynomial of the adjacency matrix for graphs using subgraphs. It also employs the use of elementary figures and basic figures to achieve these counts.

An *elementary figure* is a circle on n vertices where $n \geq 2$, a P_1 subgraph, or an isolated vertex. A *basic figure* U is the disjoint union of elementary figures.

Let $\mathscr{U}_k$ be the set of all basic figures in G with exactly k isolated vertices. Let $p(U)$ be the number of elementary figures of U and let $c(U)$ denote the number of circles in U. Given this information for a graph G and the adjacency matrix $\mathbf{A}$ of G, Sachs' Theorem finds the coefficients of the characteristic polynomial of $\mathbf{A}$.

Theorem 2.2.6 (Sachs' Theorem) *For a graph G with $n = |V(G)|$,*

$$\chi_G(\mathbf{A}, x) = \sum_{k=1}^{n}\left(\sum_{U\in\mathscr{U}_k}(-1)^{p(U)}(2)^{c(U)}\right)x^k.$$

Example 2.2.7 *Consider the basic figures of Figure 1 shown in Figure 11.*

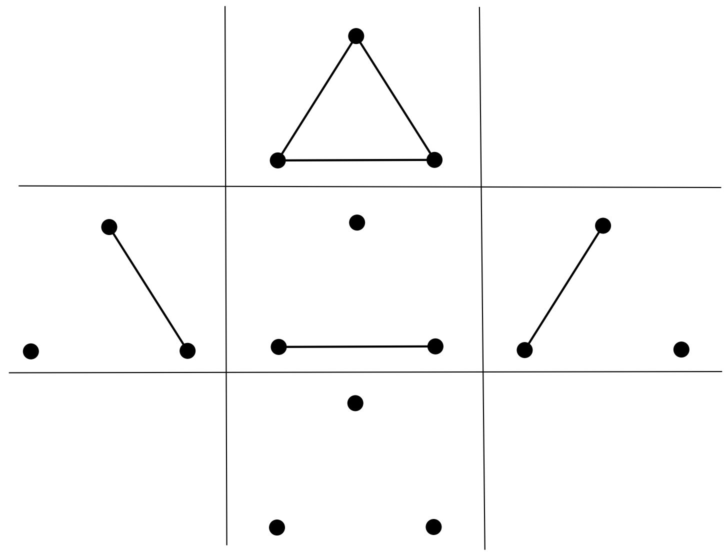

Figure 11: The set of basic figures for the graph in Figure 1.

We will use these figures to examine the constant term of the characteristic polynomial via Sachs' Theorem.

$$\begin{aligned}\det(x\mathbf{I}-\mathbf{A}) &= \det\begin{bmatrix} x & -1 & -1 \\ -1 & x & -1 \\ -1 & -1 & x \end{bmatrix} \\ &= (x)(x^2-1)+(-x+-1)-(1+x) \\ &= x^3-3x-2\end{aligned}$$

From the set of basic figures in Figure 11, there is only one where no vertices are isolated and it is an elementary figure containing one circle. Thus Sachs' Theorem calculates the coefficient of x^0 *to be* $(-1)^1(2)^1=-2$ *which is the constant term of the characteristic polynomial of the adjacency matrix of the graph.*

2.3 Contributors

In this section, we will refine the concept of permutations via an embedded path map. To begin, we define specific subgraph configurations and then define contributors, which form the foundation for the results in all further sections of this thesis.

A *contributor of* G is an incidence preserving map from a disjoint union of $\vec{P}_1$'s into G defined by $c : \coprod_{v \in V} \vec{P}_1 \to G$ such that $c(t_v) = v$ and $\{c(h_v) \mid v \in V\} = V$. Let $\mathfrak{C}(G)$ denote the set of contributors. A *strong contributor of* G is a incidence-monic contributor. Notice strong contributors are orientations of basic figures. Let $\mathfrak{S}(G)$ denote the set of strong contributors. An *identity contributor of* G is a contributor that only contains backsteps.

Example 2.3.1 *Consider the graph in Figure 1. There are sixteen different contributors of the graph.*

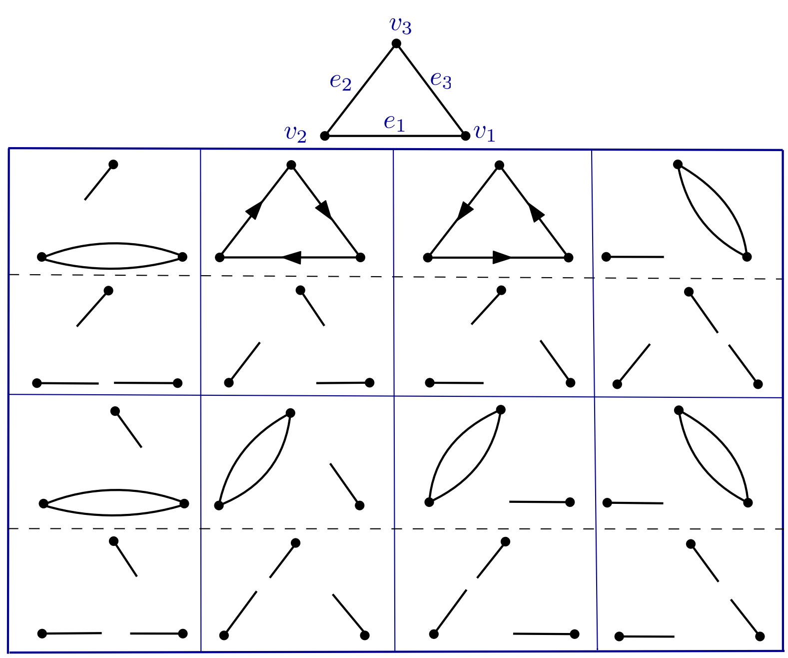

Figure 12: The contributors of a three edge, three vertex graph.

There are two strong contributors of Figure 1 and eight identity contributors.

Notice that a three edge, three vertex graph has sixteen contributors while a graph with three vertices and one hyperedge has only six contributors.

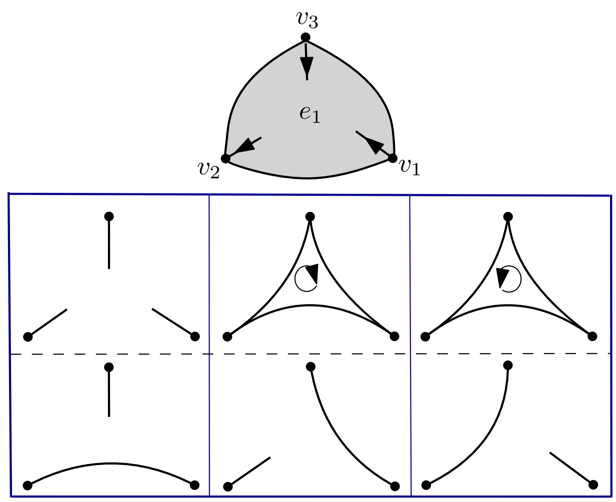

Figure 13: An orientation of a hypergraph consisting of one edge and three vertices and its six contributors.

Consider Figure 13. Like graphs, hypergraphs can be analyzed by examining their contributors. There are only six contributors and one identity contributor for the graph as seen in Figure 13.

Let $U, W \subseteq V$. The set of contributors of an oriented hypergraph is denoted $\mathfrak{C}(G)$. From here on, let $U, W \subseteq V$ with $|U| = |W|$, with a total ordering of each set denoted by $\mathbf{u}$ and $\mathbf{w}$, respectively. Let $\mathfrak{C}(G; \mathbf{u}, \mathbf{w})$ be the set of *restricted* contributors in G where $c(u_i) = w_i$, and two elements of $\mathfrak{C}(G; \mathbf{u}, \mathbf{w})$ are said to be $[\mathbf{u}, \mathbf{w}]$-*equivalent*. Let $\hat{\mathfrak{C}}(G; \mathbf{u}, \mathbf{w})$ be the set obtained by removing the $\mathbf{u} \to \mathbf{w}$ mappings from $\mathfrak{C}(G; \mathbf{u}, \mathbf{w})$; the elements of $\hat{\mathfrak{C}}(G; \mathbf{u}, \mathbf{w})$ are called the *reduced* $[\mathbf{u}, \mathbf{w}]$-equivalent contributors.

A (U, W)-*restricted contributor of* G is an incidence preserving map from a disjoint union of $\overrightarrow{P}_1$'s into G defined by $c : \coprod_{u \in U} \overrightarrow{P}_1 \to G$ such that $c(t_u) = u$ and $\{c(h_u) \mid u \in U\} = W$.

Example 2.3.2 *Figure 14 shows four contributors of the hypergraph G from Figure 9. The tail of each path is labeled with a different shape and mapped to its corresponding vertex in G; the heads are then mapped to cover the vertex set again. The bottom two contributors consist of all backsteps and are clones of the identity permutation. Identity permutation clones are distinct contributors regardless of the fact that the permutation is the same.*

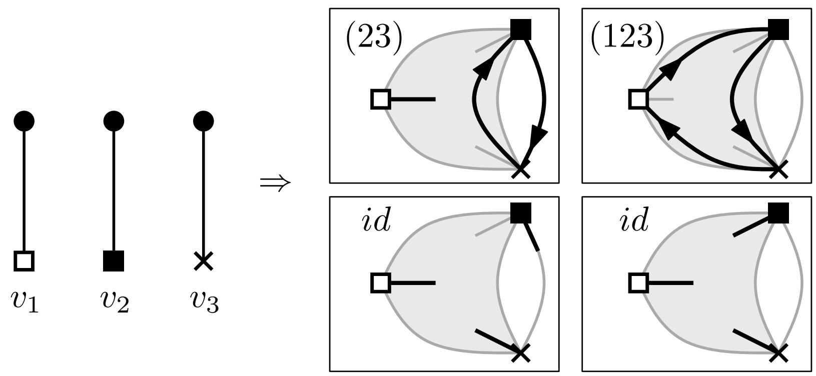

Figure 14: Contributor examples with associated permutations.

The contributors above each identity-clone are $[v_2, v_3]$-equivalent as there is a path mapping to the v_2v_3-adjacency in each contributor.

2.4 Generalized Characteristic Polynomials

Based on the concept of characteristic polynomials, there are a variety of prior theorems that have informed the research presented in this thesis. We begin with the Total Minor Polynomial and continue with variations of Matrix-tree Theorems in Section 2.5.

Before stating the Total Minor Polynomial, we present two theorems that inform it. First, the calculation of determinants and permanents based on contributors, and, second, the characteristic polynomial calculation from contributors.

Theorem 2.4.1 *Let G be an oriented hypergraph with adjacency matrix $\mathbf{A}_G$ and Laplacian matrix $\mathbf{L}_G$, then*

1. $\operatorname{perm}(\mathbf{L}_G) = \sum_{c \in \mathfrak{C}_{\geq 0}(G)} (-1)^{oc(c)+nc(c)}$,

2. $\det(\mathbf{L}_G) = \sum_{c \in \mathfrak{C}_{\geq 0}(G)} (-1)^{pc(c)}$,

3. $\operatorname{perm}(\mathbf{A}_G) = \sum_{c \in \mathfrak{C}_{=0}(G)} (-1)^{nc(c)}$,

4. $\det(\mathbf{A}_G) = \sum_{c \in \mathfrak{C}_{=0}(G)} (-1)^{ec(c)+nc(c)}$.

Calculating the minors from Theorem 2.4.1, a generalization of Sachs' Theorem in Theorem 2.4.2, was done by [6].

Theorem 2.4.2 *Let G be an oriented hypergraph with adjacency matrix $\mathbf{A}_G$ and Laplacian matrix $\mathbf{L}_G$, then*

1. $\chi^P(\mathbf{A}_G, x) = \sum_{k=0}^{|V|} \left(\sum_{c \in \hat{\mathfrak{C}}_{=k}(G)} (-1)^{oc(c)+nc(c)} \right) x^k$,

2. $\chi^D(\mathbf{A}_G, x) = \sum_{k=0}^{|V|} \left(\sum_{c \in \hat{\mathfrak{C}}_{=k}(G)} (-1)^{pc(c)} \right) x^k$,

3. $\chi^P(\mathbf{L}_G, x) = \sum_{k=0}^{|V|} \left(\sum_{c \in \hat{\mathfrak{C}}_{\geq k}(G)} (-1)^{nc(c)+bs(c)} \right) x^k$,

4. $\chi^D(\mathbf{L}_G, x) = \sum_{k=0}^{|V|} \left(\sum_{c \in \hat{\mathfrak{C}}_{\geq k}(G)} (-1)^{ec(c)+nc(c)+bs(c)} \right) x^k$.

The *zero-loading of G*, denoted $L^0(G)$, extends the hypergraph to a uniform hypergraph through the incidence structure and assigns a weight of 0 to all new incidences. This loading allows for the Total Minor Polynomial Theorem presented below.

Theorem 2.4.3 ([12], Theorem 3.1.2) *Let G be an oriented hypergraph with Laplacian matrix $\mathbf{L}_G$, then*

1. $$\chi^P(\mathbf{L}_G,\mathbf{x}) = \sum_{[\mathbf{u},\mathbf{w}]}\left(\sum_{\substack{c\in\hat{\mathfrak{C}}(L^0(G);\mathbf{u},\mathbf{w})\\ \mathrm{sgn}(c)\neq 0}}(-1)^{nc(c)+bs(c)}\right)\prod_i x_{u_i,w_i},$$

2. $$\chi^D(\mathbf{L}_G,\mathbf{x}) = \sum_{[\mathbf{u},\mathbf{w}]}\left(\sum_{\substack{c\in\hat{\mathfrak{C}}(L^0(G);\mathbf{u},\mathbf{w})\\ \mathrm{sgn}(c)\neq 0}}(-1)^{ec(\check{c})+nc(c)+bs(c)}\right)\prod_i x_{u_i,w_i}.$$

where $ec(\check{c})$ represents the number of even-cycles in the unreduced contributor of c, $bs(c)$ represents the number of backsteps, and $nc(c)$ represents the number of negative components.

Example 2.4.4 *Consider the graph in Figure 13 and its contributors.*

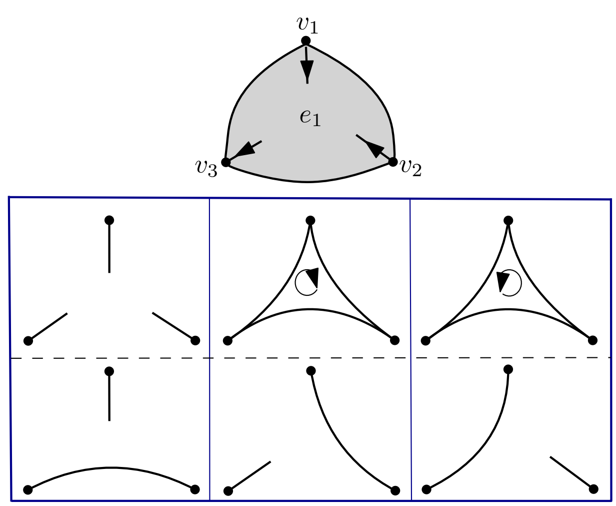

Figure 15: There are six contributors for the hypergraph in Figure 13.

The determinant of its Laplacian subtracted from $\mathbf{X}$ yields the following polynomial.

$$\det(\mathbf{X}-\mathbf{L}) \quad = \quad \det\begin{bmatrix} x_{11}-1 & x_{12}-1 & x_{13}+1 \\ x_{21}-1 & x_{22}-1 & x_{23}+1 \\ x_{31}+1 & x_{32}+1 & x_{33}-1 \end{bmatrix}$$

$$
\begin{aligned}
= \quad & x_{11}x_{22}x_{33} - x_{11}x_{23}x_{32} - x_{13}x_{22}x_{31} - x_{12}x_{21}x_{33} \\
+ \quad & x_{12}x_{23}x_{31} + x_{13}x_{21}x_{32} \\
- \quad & x_{11}x_{22} - x_{11}x_{23} - x_{11}x_{32} - x_{11}x_{33} - x_{13}x_{22} - x_{22}x_{31} \\
- \quad & x_{22}x_{33} + x_{12}x_{21} + x_{13}x_{21} + x_{12}x_{23} + x_{12}x_{31} + x_{13}x_{31} \\
- \quad & x_{23}x_{31} - x_{13}x_{32} + x_{21}x_{32} + x_{23}x_{32} \\
+ \quad & x_{12}x_{33} + x_{12}x_{33} \\
+ \quad & 0x_{11} + 0x_{22} + 0x_{33}
\end{aligned}
$$

To save space, only the x_{ij} terms along the diagonal are listed, as all the single x terms have a coefficient of zero. To find the coefficient of x_{11}, examine the two contributors in 15 with the backstep on vertex one. Once this backstep is removed, the sign of the contributor can be calculated. The contributor with all backsteps shows up as a positive contributor, since it is negative one squared, and the contributor without any backsteps, once the backstep on vertex one is removed, has an even circle and will show up as negative in the calculation. The alternating signs on the contributors account for why in this example the single x terms are zero.

2.5 Matrix-tree Theorems

Matrix-tree Theorem calculations are based on spanning trees of a graph through examining minors of Laplacians. These theorems, despite having come before the Total Minor polynomial, are in many ways specializations of it.

Theorem 2.5.1 (Tutte's Matrix-tree Theorem [22]) *If v is a vertex of a graph G, with Laplacian matrix $\mathbf{L}(G)$ then*

$$\det(\mathbf{L}_v(G)) = \sum_T \prod_{e \in E(T)} wt(e),$$

where the sum is over all spanning trees T, rooted at v, and $wt(e)$ is the weight of edge e.

In [5], Seth Chaiken generalized the Matrix-tree Theorem to all minors for signed graphs.

Theorem 2.5.2 (Seth Chaiken's All Minors Matrix-tree Theorem [5]) *Let G be a signed graph with Laplacian matrix $\mathbf{L}$. For $U, W \subseteq V$ with $|U| = |W|$, let $\mathbf{L}_{U,W}$ be (U, W) minor of $\mathbf{L}$ then*

$$\det(\mathbf{L}_{U,W}) = \epsilon(\bar{U}, V)\epsilon(\bar{W}, V) \sum_{F} \epsilon(\pi^*)(-1)^{np(F)} 4^{nc(F)} a_F,$$

where the sum is over all edge sets F, subset of E, such that

1. *F contains $|U|$ components that are trees.*

2. *Each tree from 1 contains exactly one vertex from U and one vertex from W.*

3. *Each tree from 1 is rooted at its vertex in U and contains exactly one vertex of W. This defines a linking $\pi^* : W \to U$. $\epsilon(\pi^*)$ is negative one to the number of inversions of π^*, and $np(F)$ is the number of negative paths in π^*.*

4. *Each of the remaining components of F contains exclusively a backstep or exactly one negative circle. $nc(F)$ is the number of negative circles.*

5. $\epsilon(\bar{U}, V) = (-1)^{|\{(i,j) | i < j, i \in U, j \in \bar{U}\}|}$

Theorem 2.5.3 (Matrix-tree Theorem) *Let G be a connected graph with Laplacian $\mathbf{L}$ and ij-minor of $\mathbf{L}_{ij}$.*

$$\det(\mathbf{L}_{ij}) = (-1)^{i+j} T(G)$$

Example 2.5.4 *Using the graph in Figure 1, we find the Laplacian and its* $\mathbf{L}_{11}$ *minor.*

$$\mathbf{L} = \begin{bmatrix} 2 & -1 & -1 \\ -1 & 2 & -1 \\ -1 & -1 & 2 \end{bmatrix}, \quad \mathbf{L}_{11} = \begin{bmatrix} 2 & -1 \\ -1 & 2 \end{bmatrix}.$$

The determinant of the $\mathbf{L}_{11}$ *minor is* $(2)(2) - (-1)(-1) = 4 - 1 = 3$. *In Figure 16, we show all three spanning trees.*

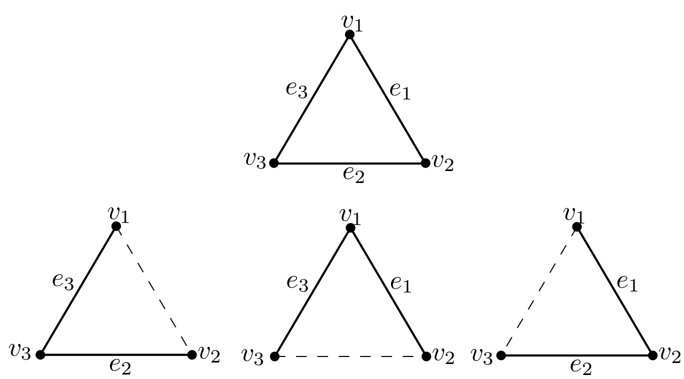

Figure 16: There are three spanning trees each with three possible roots.

The tree number of the graph is three and $i + j = 1 + 1 = 2$ *and* $(-1)^{i+j}T(G) = (-1)^2(3) = 3$. *According to the Matrix-tree Theorem, the determinant of the* $\mathbf{L}_{11}$ *minor is equal to the tree number with the appropriate sign adjustment.*

From the above example, we can observe that spanning trees are just specific contributors, and thus the calculations for the Matrix-tree Theorems are restrictions of the total minor polynomial.

3 KIRCHHOFF'S LAWS

In this section, we will examine how contributors can be used to extend Kirchhoff's Laws to signed graphs. First, we will examine transpedances and the work done in [4]. From here, we will define classes of contributors in Section 3.2, utilize these contributor transpedances to discuss arborescences in Section 3.2.1, and then redefine transpedances as contributors in Section 3.2.2. Combining these results, we will be able to define transpedance evaluations in Section 3.3. Finally, we will discuss contributor sorts via source-sink paths in Section 3.4.

3.1 Transpedances

In this section, we address how contributors are used to extend Kirchhoff's Laws to signed graphs.

We begin in Section 3.2 with classes of contributors, which will also be used in the refinement of Hadamard's Conjecture. In the next few sections, we examine contributor arborescences, transpedances, and contributors as transpedances. Finally, in Sections 3.3 and 3.4, we discuss the evaluation of transpedances and how they relate to paths within the graph.

Kirchhoff's Laws, with unit resistance, have been shown to be equivalent to 2-arborescence counts whose values are commensurable with the tree number of the graph [4]. Non-unit resistance is simply a weighted version of this combinatorial result, while directed graphs produce a non-conservative version of Kirchhoff's Laws [22]. We will show that contributor mappings produce adjacency labelings and a non-conservative generalization of Kichhoff's Laws for signed graphs.

Let $u_1, u_2, w_1, w_2 \in V(G)$, and define $\langle u_1w_1, u_2w_2\rangle$ be the number of 2-arborescences with one component rooted at u_1 and containing w_1, and the other component rooted at u_2 and containing w_2.

Given graph G with source u_1 and sink u_2, the w_1w_2-*transpedance* of G is

$$[u_1u_2, w_1w_2] = \langle u_1w_1, u_2w_2\rangle - \langle u_1w_2, u_2w_1\rangle.$$

It was shown in [4, 22] that the value $[u_1u_2, w_1w_2]$ is also the second (ordered) cofactor of the Laplacian of G. Let $\mathbf{L}_G$ be the Laplacian of G, let $\mathbf{L}_{(G;u_1,w_1)}$ be the u_1w_1-minor of L, let $\mathbf{L}_{(G;u_1u_2,w_1w_2)}$ be the u_2w_2-minor of $\mathbf{L}_{(G;u_1,w_1)}$, and define $\mathbf{L}_{(G;\mathbf{u},\mathbf{w})}$ iteratively for vertex vectors $\mathbf{u}, \mathbf{w}$. Specifically, $[u_1u_2, w_1w_2]$ is the value of the u_2w_2-cofactor in the u_1w_1-minor using the positional sign of u_1w_1 in $\mathbf{L}_G$ and the positional sign of u_2w_2 in $\mathbf{L}_{(G;u_1,w_1)}$.

Example 3.1.1 *As seen in Figure 17, there are no* 2*-arborescences of the form* $\langle v_5v_1, v_4v_6\rangle$ *because we cannot place* v_5 *and* v_1 *in a component that is disjoint from a component containing* v_6 *and* v_4*. Thus, a transpedance value of* $[v_5v_4, v_6v_1] = 4$ *is assigned to the edge between* v_5 *and* v_6*. Note that transpedances are directional, so* $[v_5v_4, v_6v_1]$ *can be regarded as the potential drop from* v_6 *to* v_1 *with source* v_5 *and sink* v_4*. Thus,* $[v_5v_4, v_1v_6]$ *would be* -4*, but it would be calculated from a different set of* 2*-arborescences.*

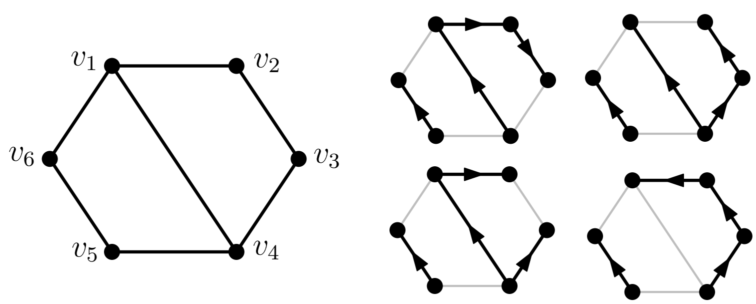

Figure 17: All 2-arborescences of the graph of the form $\langle v_5v_6, v_4v_1\rangle$.

The edge labelings produced by transpedances yield the following theorem of combinatorial Kirchhoff's Laws.

Theorem 3.1.2 ([4, 22]) *Let G be a graph with tree number $\tau(G)$, the following hold:*

1. *(Degeneracy)* $[u_1u_1, w_1w_2] = [u_1u_2, w_1w_1] = 0$,
2. *(Energy Reversal)* $[u_1u_2, w_1w_2] = -[u_1u_2, w_2w_1] = -[u_2u_1, w_1w_2]$,
3. *(Cycle Conservation)* $[u_1u_2, w_1w_2] + [u_1u_2, w_2w_3] + [u_1u_2, w_3w_1] = 0$,
4. *(Vertex Conservation)* $\sum_{y:y\sim w_1} l_{vy}[u_1u_2, w_1y] = \tau(G)\delta_{u_2w_1} - \tau(G)\delta_{u_1w_1}$,

where $\delta_{uw} = 1$ if $u = w$, and is 0 otherwise.

The above theorem establishes that degenerate transpedances have a value of 0, flow reversal causes negation, and path concatenation, cycle-conservation, and vertex-conservation (with the exception of the source and sink) hold. There is a natural flow of $\tau(G)$ out of the source and into the sink.

Example 3.1.3 *The transpedance labeling of the graph in Figure 17 with source v_5 and sink v_4 appears in Figure 18. The four 2-arborescences in Figure 17 are assigned to the directed adjacency between v_6 and v_1.*

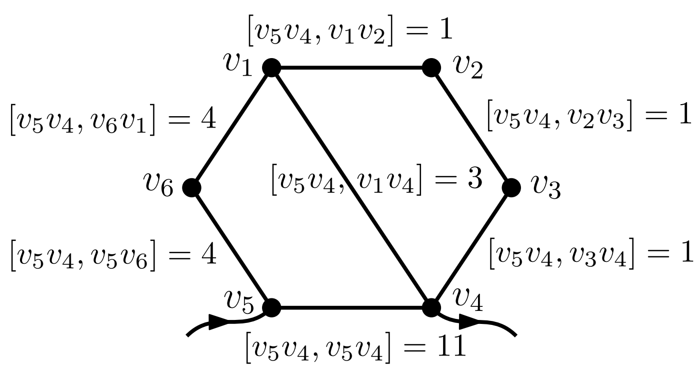

Figure 18: A transpedance labeling of G with source v_5 and sink v_4

Observe that directed cycle sums relative to source v_5 and sink v_4 are zero. Also, the in/out vertex sums are zero — with the exception of the source and sink, whose values are the tree number 15. The total in and out flow of the graph, from v_5 to v_4, is represented by the 15 spanning trees.

We have already shown that arborescences are contributors and in the following sections we will show how this relationship will allow the extension of Kirchhoff's Laws to signed graphs.

3.2 Tail-Equivalence and Contributor Classes

In this section, we will discuss concepts that are important for both Kirchoff's Laws and the examination of Hadamard's Conjecture in Section 5.

Two contributors are *tail-equivalent* if the image of their tail-incidences agree. Clearly, each tail-equivalence class has a single identity contributor containing only backsteps. The elements of a tail-equivalence class are partially ordered by $c \leq c'$ if (1) the set of circles of c is contained in the set of circles of c', or (2) the set of incidences are equal and c has more connected components than c'. Thus, the identity-contributor, having the most components and an empty set of circles, is the least element of each poset. Two examples appear in Figure 19.

Tail-equivalence is a generalization of the work in circle activation classes on bidirected graphs in [20]. *Unpacking* is the act of extending a backstep into its unique directed adjacency, and *packing* is the folding of a directed adjacency back into a backstep. For bidirected graphs, these two operations are well-defined and have inverses. However, in oriented hypergraphs only packing is well-defined, as edges can have more than two incidences mapped to them. Contributors that are packing/unpacking equivalent are grouped into *activation classes* and ordered as new circles appear.

Example 3.2.1 *Each identity-contributor in the figure below is tail-equivalent to the contributors above them as each $\overrightarrow{P_1}$ maps to the same initial incidence.*

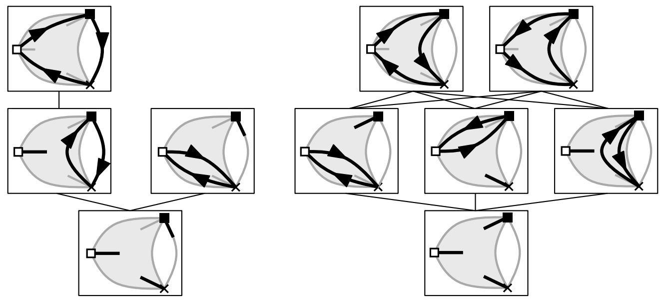

Figure 19: Tail-equivalence classes from Figure 14.

Let $\mathcal{A}(G)$ denote a tail-equivalence class of G. For bidirected graphs, we will follow the convention of referring to the tail-equivalence classes as activation classes, where two contributors are clearly in the same activation class if they are packing or unpacking equivalent. As with restricted and reduced contributors, we let $\mathcal{A}(\mathbf{u};\mathbf{w};G)$ be the elements of tail-equivalency class $\mathcal{A}(G)$ where $u_i \mapsto w_i$, and $\hat{\mathcal{A}}(\mathbf{u};\mathbf{w};G)$ be the elements of $\mathcal{A}(\mathbf{u};\mathbf{w};G)$ with $u_i \mapsto w_i$ removed for each i. From [20], the activation classes and their restricted subclasses of a bidirected graph are Boolean lattices.

Lemma 3.2.2 ([20], Lemma 3.6) *For a bidirected graph G, all activation classes of G are Boolean lattices.*

Furthermore, it was shown in [12] that the reduced contributors in single element activation classes, $\hat{\mathcal{A}}_{\neq 0}(\mathbf{u};\mathbf{w};L^0(G))$, are unpacking equivalent to k-arborescences.

Theorem 3.2.3 ([12], Theorem 3.2.4) *In a bidirected graph G the set of all elements in single-element $\hat{\mathcal{A}}_{\neq 0}(\mathbf{u};\mathbf{w};L^0(G))$ are unpacking equivalent to k-arborescences. Moreover, the i^{th} component in the arborescence has sink u_i, and the vertices of each component are determined by the linking induced by c^{-1} between all $u_i \in U \cap \overline{W} \to \overline{U}$ or unpack into a vertex of a linking component.*

Given the importance of single-element trivial activation classes, which will appear repeatedly, let $\hat{\mathfrak{C}}^1_{\neq 0}(L^0(G); u_1u_2, w_1w_2)$ be the non-zero elements of $\hat{\mathfrak{C}}(L^0(G); u_1u_2, w_1w_2)$ in trivial activation classes.

Example 3.2.4 *Consider the graph from Figure 17. Each of the identity-contributors have no circles, so the backsteps may be unpacked to produce new cycles. Since every edge contains a unique adjacency, the contributors are ordered by their circle sets. The subclass where $v_i \mapsto v_j$ is an order ideal. Three activation classes appear in Figure 20 along with their $v_5 \mapsto v_4$ subclasses highlighted. The top contributor in the rightmost figure in Figure 20 is a trivial $v_5 \mapsto v_4$ subclass. Additionally, the removal of the $v_5 \mapsto v_4$ map leaves a rooted spanning tree which is equivalent to* 1*-arborescences.*

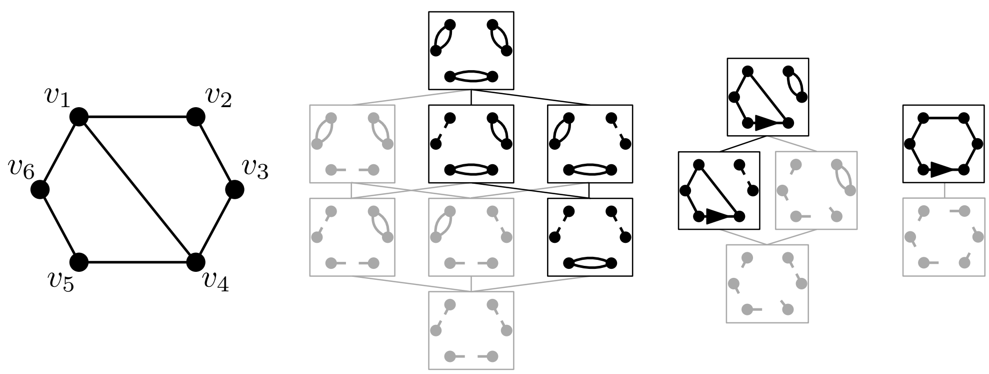

Figure 20: Three Boolean activation classes for the given graph and their $v_5 \mapsto v_4$ activation subclass (darker).

To see how a 2*-arborescence is formed, consider the middle activation class in Figure 20 where $v_5 \mapsto v_4$. Remove the $v_5 \mapsto v_4$ map, then take the second order ideal induced by $v_2 \mapsto v_3$ — this gives the middle contributors in Figure 21. The removal of the $v_2 \mapsto v_3$ mapping and unpacking of any backsteps yields the* 2*-arborescence on the right of Figure 21.*

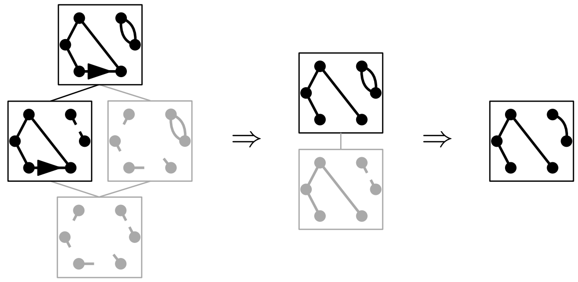

Figure 21: A trivial $[v_5v_2, v_4v_3]$-reduced activation class unpacks into a 2-arborescence.

3.2.1 Contributor Arborescences

The 2-arborescences that arise from trivial activation classes need not be the same as Tutte's. A 2-arborescence for the transpedance calculation $[u_1u_2, w_1w_2]$ will be called a *Tutte-2-arborescence* while a 2-arborescence described as an element of $\hat{\mathfrak{C}}^1_{\neq 0}(L^0(G); u_1u_2, w_1w_2)$ will be called a *contributor-2-arborescence.*

Let F be a Tutte-2-arborescence in the calculation of $[u_1u_2, w_1w_2]$; the sign of F (relative to $[u_1u_2, w_1w_2]$), denoted $sgn_T(F)$, is +1 if it contributes to the value of $\langle u_1w_1, u_2w_2\rangle$ and −1 if it contributes to the value of $\langle u_1w_2, u_2w_1\rangle$. Tutte and contributor-2-arborescences are related via the Linking Lemma and the number of cycles that are formed.

Lemma 3.2.5 *There is a bijection between Tutte-2-arborescences of the form $[u_1u_2, w_1w_2]$ and contributor-2-arborescences from $\hat{\mathfrak{C}}^1_{\neq 0}(L^0(G); u_1u_2, w_1w_2)$.*

Proof. Let u_1 and u_2 be the source and sink, respectively, and let w_1 and w_2 be two vertices.

Part I: Let F be a Tutte-2-arborescence for $[u_1u_2, w_1w_2]$. There are two cases based on $sgn_T(F)$.

Case 1 ($sgn_T(F) = +1$): If $sgn_T(F) = +1$, then u_1 and w_1 are in one component, and u_2 and w_2 are in the other. Reverse the path from u_1 and w_1 and u_2 and w_2 within each component. Introduce edges directed $u_1 \mapsto w_1$ and $u_2 \mapsto w_2$ to complete two disjoint cycles. Note that these edges need not exist in G as they exist in the zero-loading and will be removed in the reduced contributor. Next, pack all adjacencies away from each cycle into backsteps and remove the $u_1 \mapsto w_1$ and $u_2 \mapsto w_2$ adjacencies. Since there are no more circles, the resulting object is in $\hat{\mathfrak{C}}^1_{\neq 0}(L^0(G); u_1u_2, w_1w_2)$.

Case 2 ($sgn_T(F) = -1$): If $sgn_T(F) = -1$, then u_1 and w_2 are in one component, and u_2 and w_1 are in the other. This is identical to case 1, except the introduction of edges directed $u_1 \mapsto w_1$ and $u_2 \mapsto w_2$ to form one cycle.

Part II: Let $c \in \hat{\mathfrak{C}}^1_{\neq 0}(L^0(G); u_1u_2, w_1w_2)$ and let $\check{c} \in \mathfrak{C}(L^0(G); u_1u_2, w_1w_2)$ be the unreduced contributor for c. Since c is in a trivial activation class, $\check{c}$ must either (a) contain 2 circles with $u_1 \mapsto w_1$ or $u_2 \mapsto w_2$ belonging to different circles, or (b) contain 1 circle with $u_1 \mapsto w_1$ and $u_2 \mapsto w_2$ belonging to the same circle.

Case 1 (Two-circles): Suppose $\check{c}$ has exactly 2-circles. First, unpack all backsteps of c, then re-introduce $u_1 \mapsto w_1$ and $u_2 \mapsto w_2$ to complete the two circles. Reverse the circle orientations and remove the adjacencies. The result is a Tutte-2-arborescence F of the form $\langle u_1w_1, u_2w_2\rangle$ and $sgn_T(F) = +1$.

Case 2 (One-circle): Again, this is similar to case 1, except the adjacencies introduced form a single circle. The result is a Tutte-2-arborescence F of the form $\langle u_1w_2, u_2w_1\rangle$, and $\mathrm{sgn}_T(F) = -1$. ■

Example 3.2.6 *Consider the top left Tutte-2-arborescence from Figure 17 in the calculation for* $[v_5v_4, v_6v_1]$. *This Tutte-2-arborescence appears on the left of Figure 22.*

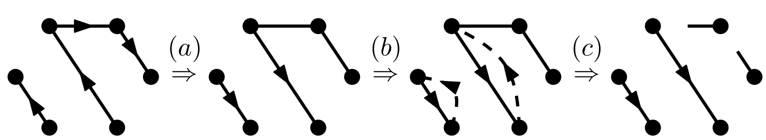

Figure 22: A Tutte-2-arborescence transforming into a reduced contributor.

The paths within each part of the arborescence are reversed in step (a). *The* *missing edge is added to produce a unique (directed) circle in step (b). Next, all edges connected to each circle via a path are packed into backsteps away from each circle, producing the original restricted contributor. Finally, the introduced edges are removed to produce the reduced contributor in step (c).*

Corollary 3.2.7 *Let F be a Tutte-2-arborescence in the calculation of $[u_1u_2, w_1w_2]$ and c_F be its corresponding element in $\hat{\mathfrak{C}}^1_{\neq 0}(L^0(G); u_1u_2, w_1w_2)$, then*

1. *$sgn_T(F) = +1$ if, and only if, $\check{c}_F$ has exactly two cycles,*
2. *$sgn_T(F) = -1$ if, and only if, $\check{c}_F$ has exactly one cycle.*

The above corollary is obtained from the proof of Lemma 3.2.5.

Corollary 3.2.8 *Let e be the edge between w_1 and w_2. Introducing the w_1w_2-edge to any Tutte-2-arborescence associated to $[u_1u_2, w_1w_2]$ or a contributor-2-arborescence associated to an element of $\hat{\mathfrak{C}}^1_{\neq 0}(L^0(G); u_1u_2, w_1w_2)$ produces a spanning tree in $G \cup e$.*

Proof. In either type of 2-arborescence w_1 and w_2 are in different components and each component is a tree. If e is an edge of G a spanning tree of G is produced. If e does not exist in G, a spanning tree in $G \cup e$ is produced. ■

Example 3.2.9 *Consider the graph in Figure 17. Two of the reduced contributors in $\hat{\mathfrak{C}}^1_{\neq 0}(L^0(G); v_5v_4, v_6v_1)$ that correspond to $[v_5v_4, v_6v_1]$ appear on the left of Figure 23. The middle figures are obtained by unpacking backsteps to produce a contributor-2-arborescence. Finally, the introduction of the v_6v_1-edge yields a spanning tree.*

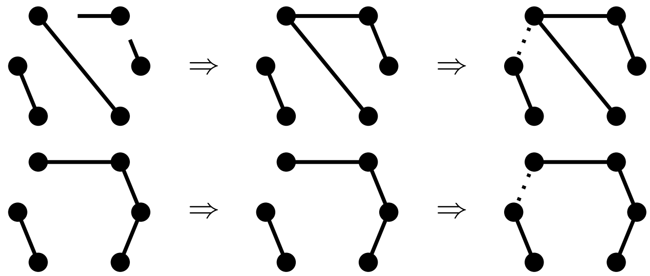

Figure 23: Trivial activation classes unpack into 2-arborescences, and those used for edge labeling produce spanning trees.

Now that we have defined contributors as arborescences, we will see in the next section that we can replace the Tutte-2-arborescences with entire contributor sets and then characterize their contributor class signs.

3.2.2 Contributors as Transpedances

In this section, we will show that edge-labeling of signed contributors provide a generalization of transpedances and Kirchhoff-type Laws to signed graphs via the coefficients of the degree-2 monomials $x_{u_1w_1}x_{u_2w_2}$ from Theorem 2.4.3.

The *determinant-sign* of a contributor c is taken from Theorem 2.4.3, where

$$sgn_D(c) = (-1)^{ec(\check{c})+nc(c)+bs(c)}.$$

The contributor-based transpedance for the determinant, or *D-contributor-transpedance*, is defined as

$$[u_1u_2, w_1w_2]_D = \sum_{c \in \hat{\mathfrak{C}}_{\neq 0}(L^0(G); u_1u_2, w_1w_2)} sgn_D(c),$$

and consider the labeling of each w_1w_2-edge with the signed contributors from $[u_1u_2, w_1w_2]_D$ when w_1 and w_2 are adjacent.

Example 3.2.10 *Again, consider the graph in Figure 17. The set of contributors that determine* $[v_5v_4, v_6v_1]_D$*, grouped into their activation classes, are shown in Figure 24.*

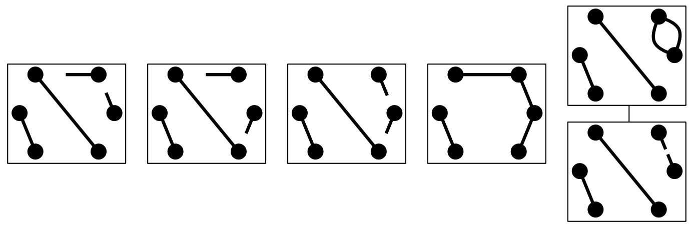

Figure 24: All activation classes for $[v_5v_4, v_6v_1]_D$.

Note that non-trivial classes sum to zero if all edges are positive, and only the trivial classes will determine $[v_5v_4, v_6v_1]_D$ *if* G *is a graph.*

The lemma below shows the simple relationship between the signs of a Tutte-2-arborescence and their associated reduced contributor.

Lemma 3.2.11 *Let* F *be a Tutte-2-arborescence and* c_F *be its corresponding element in* $\hat{\mathfrak{C}}^1_{\neq 0}(L^0(G); u_1u_2, w_1w_2)$*, then* $sgn_T(F) = (-1)^{|V|} sgn_D(c_F)$.

Proof.

Tutte's transpedances $[u_1u_2, w_1w_2]$ are ordered second cofactors from the Laplacian $\mathbf{L}_{(G;u_1u_2,w_1w_2)}$, and the Tutte-2-arborescences are the signed commensurable parts that sum to $[u_1u_2, w_1w_2]$. From Theorem 2.4.3, the coefficient of $x_{u_1w_1}x_{u_2w_2}$ is $[u_1u_2, w_1w_2]_D$, and the reduced contributors are the signed commensurable parts that sum to $[u_1u_2, w_1w_2]_D$, but the coefficient of $x_{u_1w_1}x_{u_2w_2}$ is determined from $\mathbf{X} - \mathbf{L}_G$. The two adjacencies removed in each reduced contributor are mapped to $x_{u_1w_1}$ and $x_{u_2w_2}$, while all $|V| - 2$ remaining Laplacian entries are negated; thus the sign discrepancy is $(-1)^{|V|-2} = (-1)^{|V|}$. ■

Tutte's transpedance degeneracy and energy reversal rules from Theorem 3.1.2 hold for D-contributor-transpedances.

Lemma 3.2.12 (Contributor Degeneracy) *Let G be a signed graph with source u_1, sink u_2, and vertices w_1 and w_2, then*

$$[u_1u_1, w_1w_2]_D = [u_1u_2, w_1w_1]_D = 0.$$

Proof. The set of reduced contributors for $\hat{\mathfrak{C}}_{\neq 0}(L^0(G); u_1u_1, w_1w_2)$ and $\hat{\mathfrak{C}}_{\neq 0}(L^0(G); u_1u_2, w_1w_1)$ are both empty. The first would require two maps of the form $u_1 \mapsto w_1$ and $u_1 \mapsto w_2$, and there cannot be two tails at u_1. The second would require two maps of the form $u_1 \mapsto w_1$ and $u_2 \mapsto w_1$, and there cannot be two heads at w_1. ∎

Using the Linking Lemma on reduced contributors, since the unreduced contributors represent permutation clones of the graph, we can produce WU-paths as the circles are cut. This idea allows for the following result to be extended for D-contributor-transpedances.

Lemma 3.2.13 (Contributor Energy Reversal) *Let G be a signed graph with source u_1, sink u_2, and vertices w_1 and w_2, then*

$$[u_1u_2, w_1w_2]_D = -[u_1u_2, w_2w_1]_D = -[u_2u_1, w_1w_2]_D.$$

Proof. We show the first equality, the second is similar.

Consider $c \in \hat{\mathfrak{C}}_{\neq 0}(L^0(G); u_1u_2, w_1w_2)$ and reintroduce maps $u_1 \mapsto w_1$ and $u_2 \mapsto w_2$ to form the unreduced contributor $\check{c}$. There are two cases depending if u_1, u_2, w_1, w_2 belong to one or two circles in $\check{c}$.

Case 1 (Two circles): In this case we have that $\{u_1, w_1\}$ and $\{u_2, w_2\}$ are in disjoint circles in $\check{c}$. Remove $u_1 \mapsto w_1$ and $u_2 \mapsto w_2$ in $\check{c}$, and replace them with $u_1 \mapsto w_2$ and $u_2 \mapsto w_2$ to form a new non-zero unreduced contributor $\check{c}'$ in $\hat{\mathfrak{C}}_{\neq 0}(L^0(G); u_1u_2, w_2w_1)$ where $\{u_1, u_2, w_1, w_2\}$ are in a single circle. Since c and c' have the same adjacencies and backsteps, the sign difference between $sgn_D(c)$ and

$sgn_D(c')$ is determined by the even circle structure of their unreduced contributors. If the original circles were both even, the new single circle is even; a loss of one even circle. If the original circles were both odd, the new circle is even; a gain of one even circle. If the original circles have different parity, the new circle is odd; a loss of one even circle. In any case $sgn_D(c) = -sgn_D(c')$.

Case 2 (One circle): In this case we have that $\{u_1, u_2, w_1, w_2\}$ are in a single circle $\check{c}$. Remove $u_1 \mapsto w_1$ and $u_2 \mapsto w_2$ in $\check{c}$, and replace them with $u_1 \mapsto w_2$ and $u_2 \mapsto w_2$ to form a new non-zero unreduced contributor $\check{c}'$ in $\hat{\mathfrak{C}}_{\neq 0}(L^0(G); u_1u_2, w_2w_1)$ where $\{u_1, w_1\}$ and $\{u_2, w_2\}$ are in disjoint circles. Since c and c' have the same adjacencies and backsteps, the sign difference between $sgn_D(c)$ and $sgn_D(c')$ is determined by the even circle structure of their unreduced contributors. If the original circle is even, each new circle is odd. If the original circle is odd, each new circle is even. Thus in either case $sgn_D(c) = -sgn_D(c')$.

This process is reversible, so we have the first equality. The second equality is similar. ∎

3.3 Transpedance Evaluation

With the sign adjustment in Lemma 3.2.11, we can immediately use the elements of $\hat{\mathfrak{C}}^1_{\neq 0}(L^0(G); u_1u_2, w_1w_2)$ in place of transpedances. We will extend these results to characterize the placement of entire contributor families on edges. Let $\hat{\mathfrak{A}}(\mathbf{u}, \mathbf{w}; G)$ be the set of all reduced activation classes of the form $\hat{\mathcal{A}}(\mathbf{u}, \mathbf{w}; G)$, and let $\hat{\mathfrak{A}}^-(\mathbf{u}, \mathbf{w}; G)$ be the subset of $\hat{\mathfrak{A}}(\mathbf{u}, \mathbf{w}; G)$ such that no element contains a positive circle. The activation class transversal consisting of maximal elements is denoted by $\mathcal{M}_{\mathbf{u},\mathbf{w}}$, and $\mathcal{M}^-_{\mathbf{u},\mathbf{w}}$ is the subset of maximal elements that are positive-circle-free. Since each activation class is Boolean (Lemma 3.2.2), D-contributor-transpedances have a simple presentation via the maximal element of each activation class.

Theorem 3.3.1 *If G is a signed graph, then*

$$[u_1u_2, w_1w_2]_D = \sum_{m \in \mathcal{M}^-_{(u_1u_2, w_1w_2)}} sgn_D(m) \cdot (2)^{\eta(m)}$$

where $\eta(m)$ is the number of negative circles in maximal contributor m.

Proof.

Let G be a signed graph with distinguished source u_1, sink u_2, edge w_1w_2, and total orderings $\mathbf{u} = (u_1, u_2)$ and $\mathbf{w} = (w_1, w_2)$. Also, let $\hat{\mathfrak{A}} = \hat{\mathfrak{A}}(\mathbf{u}, \mathbf{w}; G)$, and $\hat{\mathcal{A}} = \hat{\mathcal{A}}(\mathbf{u}, \mathbf{w}; G)$. Partition the D-contributor-transpedance value $[u_1u_2, w_1w_2]_D$ into activation classes as follows:

$$\begin{aligned}[u_1u_2, w_1w_2]_D &= \sum_{\hat{\mathcal{A}} \in \hat{\mathfrak{A}}} \sum_{c \in \hat{\mathcal{A}}} sgn_D(c) \\ &= \sum_{\hat{\mathcal{A}} \in \hat{\mathfrak{A}}^-} \sum_{c \in \hat{\mathcal{A}}} sgn_D(c) + \sum_{\hat{\mathcal{A}} \in \hat{\mathfrak{A}} \smallsetminus \hat{\mathfrak{A}}^-} \sum_{c \in \hat{\mathcal{A}}} sgn_D(c)\end{aligned}$$

From Lemma 3.2.2, activation classes form Boolean lattices, and each sum is calculated separately.

Case 1 (No positive circles): Let contributors c and c' only differ by a single negative circle, which appears in c but not in c'. Let the length of this circle be ℓ. Packing this circle into backsteps will yield a loss of a single positive circle and a gain of ℓ backsteps.

Case 1a (ℓ is odd): If ℓ is odd, the $sgn_D(c')$ is related to $sgn_D(c)$ as follows:

$$\begin{aligned}sgn_D(c') &= (-1)^{ec(\check{c})+(nc(c)-1)+(bs(c)+\ell)} \\ &= (-1)^{ec(\check{c})+nc(c)+bs(c)} \cdot (-1)^{\ell-1} = sgn_D(c).\end{aligned}$$

Case 1b (ℓ is even): If ℓ is even, packing also loses an even circle and $sgn_D(c')$

is related to $sgn_D(c)$ as follows:

$$sgn_D(c') = (-1)^{(ec(\check{c})-1)+(nc(c)-1)+(bs(c)+\ell)}$$
$$= (-1)^{ec(\check{c})+nc(c)+bs(c)} \cdot (-1)^{\ell-2} = sgn_D(c).$$

Since each element has the same sign and each activation class is Boolean there are $2^{\eta(m)}$ contributors, where m is the maximal contributor containing $\eta(m)$ circles. So it follows that:

$$\sum_{\hat{\mathcal{A}} \in \hat{\mathfrak{A}}^-} \sum_{c \in \hat{\mathcal{A}}} sgn_D(c) = \sum_{m \in \mathcal{M}^-_{(u_1 u_2, w_1 w_2)}} sgn_D(m) \cdot (2)^{\eta(m)}.$$

Case 2 (Positive circle): Let contributors c and c' only differ by a single positive circle, which appears in c but not in c'. Let the length of this circle be ℓ. Packing this circle into backsteps will yield a loss of a single positive circle and a gain of ℓ backsteps.

Case 2a (ℓ is odd): If ℓ is odd, the $sgn_D(c')$ is related to $sgn_D(c)$ as follows:

$$sgn_D(c') = (-1)^{ec(\check{c})+nc(c)+(bs(c)+\ell)}$$
$$= (-1)^{ec(\check{c})+nc(c)+bs(c)} \cdot (-1)^{\ell} = -sgn_D(c).$$

Case 2b (ℓ is even): If ℓ is even, packing also loses an even circle and $sgn_D(c')$ is related to $sgn_D(c)$ as follows:

$$sgn_D(c') = (-1)^{(ec(\check{c})-1)+nc(c)+(bs(c)+\ell)}$$
$$= (-1)^{ec(\check{c})+nc(c)+bs(c)} \cdot (-1)^{\ell-1} = -sgn_D(c).$$

Again, since each activation class is Boolean, there is a bijection between contributors with circle C and those without C via packing/unpacking. Thus, each activation class that contains a contributor with a positive circle will have those contributors sum to 0. Moreover, the remaining classes are determined by the sign of their maximal element.

$$[u_1u_2, w_1w_2]_D = \sum_{\hat{\mathcal{A}}\in\hat{\mathfrak{A}}^-} \sum_{c\in\hat{\mathcal{A}}} sgn_D(c) + 0$$
$$= \sum_{m\in\mathcal{M}_{\bar{\mathbf{u}};\mathbf{w}}} sgn_D(m)\cdot(2)^{\eta(m)}.$$

■

Transpedances are second cofactors. These arise naturally as the coefficients of the degree-2 monomials of the total minor polynomial for integer matrix Laplacians [12], where the coefficients are determined by sums of reduced contributors.

Example 3.3.2 *Consider the transpedance value* $[v_5v_4, v_1v_2] = 1$ *along the top edge in Figure 18. This value can be calculated through the total minor polynomial by first finding all contributors where* $v_5 \mapsto v_1$ *and* $v_4 \mapsto v_2$*, then removing these two maps — these maps are allowed to exist in the zero-loading* $L^0(G)$*. If they do not exist in the original graph and are then subsequently removed the contributor then exists. The remaining objects need to exist in* G *to avoid mapping to* 0*. In this case, there is only one such reduced contributor that lies in* G*, shown in Figure 25.*

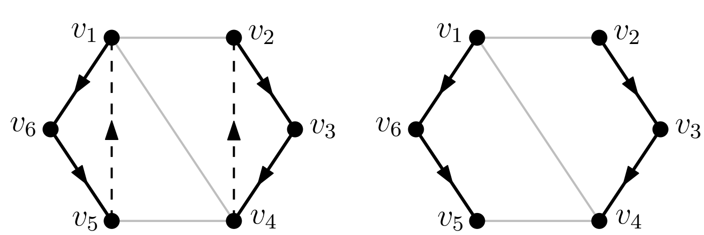

Figure 25: Reduced contributors find coefficients of the total minor polynomial as generalized cycle covers.

Using the determinant signing function in Theorem 2.4.3, and assuming every edge is positive (as in a graph) because we have not specified edge signings, we find $ec(\check{c}) = 0$ *since there are* 0 *even circles in the non-reduced contributor while* $nc(c) = 0$

and $bs(c) = 0$. *Thus, the sign of the contributor is* $(-1)^{0+0+0} = 1$. *This is the value of the coefficient of* $x_{v_5v_1}x_{v_4v_2}$ *as well as* $[v_5v_4, v_1v_2]$, *as depicted in Figure 18.*

From here we can combine Lemmas 3.2.5, 3.2.11, and Theorem 3.3.1 to find the following interpretation of Tutte-transpedances:

Corollary 3.3.3 (Parity-Polarity Reversal) *If* G *is a signed graph with all positive edges, then* $[u_1u_2, w_1w_2] = (-1)^{|V|}[u_1u_2, w_1w_2]_D$.

Proof. If all edges are positive, by Theorem 3.3.1, the only non-cancellative terms are trivial reduced activation classes. The bijection between 2-arborescence types in Lemma 3.2.5 combined with the signing in Lemma 3.2.11 completes the proof. ■

That is to say that Tutte's edge-labeling via transpedances provides a natural orientation from source to sink, where the difference lies in that the contributor version is negated for graphs where the number of vertices is odd.

For a graph with all positive edges, like Figure 20, and the contributors for $[v_5v_4, v_6v_1]_D$ in Figure 24, produce a value of +4 as the non-trivial classes sum to 0 and there is an even number of vertices. This agrees with Tutte's transpedance $[v_5v_4, v_6v_1]$.

However, a signed graph may not have their non-trivial activation classes cancel.

Example 3.3.4 *For a new example, consider the signed graph in Figure 26 with source* v_5 *and sink* v_4. *To calculate the D-contributor-transpedance along edge* v_5v_4, *we examine* $[v_5v_4, v_5v_4]_D$. *The contributors in Figure 26 are the non-cancellative contributors as they do not contain positive circles. Since there are an odd number of vertices, the value is negated relative to Tutte's and the value is* -12.

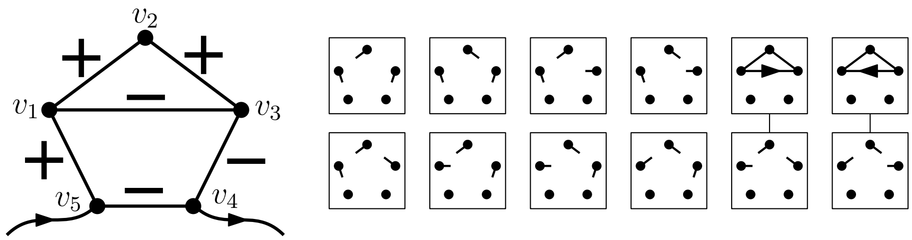

Figure 26: Non-trivial reduced-contributors signed $[v_5v_4, v_5v_4]_D = -12$

If all the edges were positive, the D-contributor-transpedance would have been -8, as the oriented 3-circles would be positive. Also, observe that there are far more than 12 contributors on edge v_5v_4. The contributors in Figure 27 always cancel as they repeat an adjacency, so the circle is always positive.

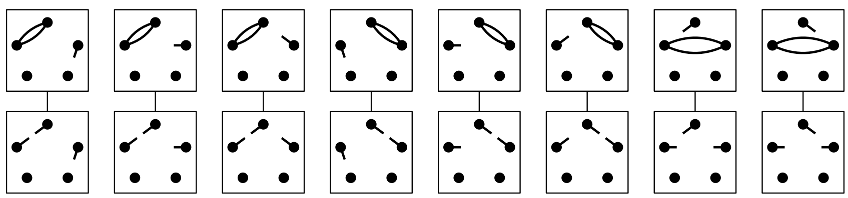

Figure 27: Non-trivial reduced-contributors signed $[v_5v_4, v_5v_4]_D = -12$

The sign between an edge does not matter when determining the D-contributor-transpedance on that edge, as the edge cannot exist in any relevant contributor. Additionally, cycles may not cancel in their activation class as they would in a graph.

3.4 Source-Sink Pathing

We have seen that contributor-transpedances satisfy their own general Degeneracy (Lemma 3.2.12) and Energy Reversal (Lemma 3.2.13) Kirchhoff-type laws. When evaluated via activation classes (Theorem 3.3.1), all positive graphs relate to Tutte-transpedances via Polarity reversal (Corollary 3.3.3). In this section, we investigate the Cycle Conservation and Vertex Conservation properties from Theorem 3.1.2 by showing that transpedances are contributor sorts along source-sink paths as a generalization of Corollary 3.2.8. However, the expectation of conservation no longer holds.

Let G be a signed graph with source u_1, sink u_2, and vertices w_1 and w_2. If w_1 and w_2 are adjacent, call their edge e. If w_1 and w_2 are not adjacent, regard G as a subgraph $G \cup e_{w_1 w_2}$ where edge $e_{w_1 w_2}$ is added between w_1 and w_2. This is called the *local-loading of* G *at* $\{w_1, w_2\}$ and is related to the injective loading properties from [13, 12]. To simplify notation, we will simply write $G \cup e_{w_1 w_2}$ with the understanding that $e_{w_1 w_2}$ may exist in G. Let $\mathcal{P}(u_1 u_2, w_1 w_2)$ be the set of $u_1 u_2$-paths containing $e_{w_1 w_2}$ in $G \cup e_{w_1 w_2}$.

Lemma 3.4.1 *A contributor c is in $\hat{\mathfrak{C}}_{\neq 0}(L^0(G); u_1 u_2, w_1 w_2)$ if, and only if, c contains a unique path $P \in \mathcal{P}(u_1 u_2, w_1 w_2)$ in $G \cup e_{w_1 w_2}$.*

Proof.

Part I: Let $c \in \hat{\mathfrak{C}}_{\neq 0}(L^0(G); u_1 u_2, w_1 w_2)$, and $\check{c}$ be its unreduced contributor. There are two cases depending if u_1, u_2, w_1, w_2 belong to one or two circles in $\check{c}$.

Case 1 (Two circles): In this case we have u_1, w_1 and u_2, w_2 are in disjoint circles in $\check{c}$. Remove $u_1 \mapsto w_1$ and $u_2 \mapsto w_2$ and reverse $u_1 \to w_1$. Note that we remove immediate adjacencies and reverse the remaining existing path from u_1 to w_1, which does not contain a adjacency between u_1 and w_1. Introduce edge e to produce a $u_1 u_2$-path P where w_1 precedes w_2 in P. Any additional circles and backsteps are external and may only extend the activation class.

Case 2 (One circle): In this case we have u_1, u_2, w_1, w_2 in a single circle in $\check{c}$. Remove $u_1 \mapsto w_1$ and $u_2 \mapsto w_2$, reverse $u_1 \to w_2$, and introduce edge e to produce a $u_1 u_2$-path P where w_2 precedes w_1 in P. Any additional circles and backsteps are external and may only extend the activation class.

Part II: Let $P \in \mathcal{P}(u_1 u_2, w_1 w_2)$. There are two cases depending if w_1 precedes w_2 or w_2 precedes w_1 in P.

Case 1 (w_1 precedes w_2): Delete $e_{w_1w_2}$, and introduce $u_1 \mapsto w_1$ and $u_2 \mapsto w_2$. Reverse the u_1w_1-part of P, and do not reverse the u_2w_2-part of P to make two circles. Introduce backsteps/circles at all remaining vertices to form an unreduced contributor $\check{c}$. Remove $u_1 \mapsto w_1$ and $u_2 \mapsto w_2$ to get $c \in \hat{\mathfrak{C}}_{\neq 0}(L^0(G); u_1u_2, w_1w_2)$. Pack/unpack as necessary to form activation classes.

Case 2 (w_2 precedes w_1): Delete $e_{w_1w_2}$, and introduce $u_1 \mapsto w_1$ and $u_2 \mapsto w_2$. Reverse the u_1w_2-part of P, and do not reverse u_2w_1-part of P to make one circle. Introduce backsteps/circles at all remaining vertices to form an unreduced contributor $\check{c}$. Remove $u_1 \mapsto w_1$ and $u_2 \mapsto w_2$ to get $c \in \hat{\mathfrak{C}}_{\neq 0}(L^0(G); u_1u_2, w_1w_2)$. Pack/unpack as necessary to form activation classes. ■

We now have the immediate corollaries demonstrating that all contributors for a given transpedance are related to a direct source-sink path property.

Corollary 3.4.2 *Let $c \in \hat{\mathfrak{C}}_{\neq 0}(L^0(G); u_1u_2, w_1w_2)$. Every edge-adjacency appearing in c outside an activated circle is in one of the parts of the w_iu_j-paths. Moreover, these paths are oriented from w_i to u_j.*

Corollary 3.4.3 *If w_1 is a monovalaent vertex that is not a source or sink with supporting edge $e_{w_1w_2}$, then $[u_1u_2, w_1w_2] = 0$.*

From here, we can observe a simple reinterpretation of Tutte's transpedances.

Corollary 3.4.4 *Let G be a graph with source u_1 and sink u_2. The edge labeling of G by transpedances $[u_1u_2, w_1w_2]$ is equivalent to a sorting of spanning trees via adjacency swapping along the u_1u_2-path in $G \cup e$.*

Proof. Corollary 3.2.8 provides an interpretation of trivial activation classes as spanning trees, even for transpedances not on adjacencies. Additionally, Corollary 3.3.3 shows that these are the only objects that do not cancel in the Boolean activation classes in a graph. Part 4 of Theorem 3.1.2 indicates the net inflow and outflow is the tree-number. ■

Example 3.4.5 *The reduced contributors in trivial activation classes for Figure 18 appear on each edge in Figure 28 (left). A source-sink path is indicated on the right with the associated unpacked contributors, shown with edges inserted to produce spanning trees on the left.*

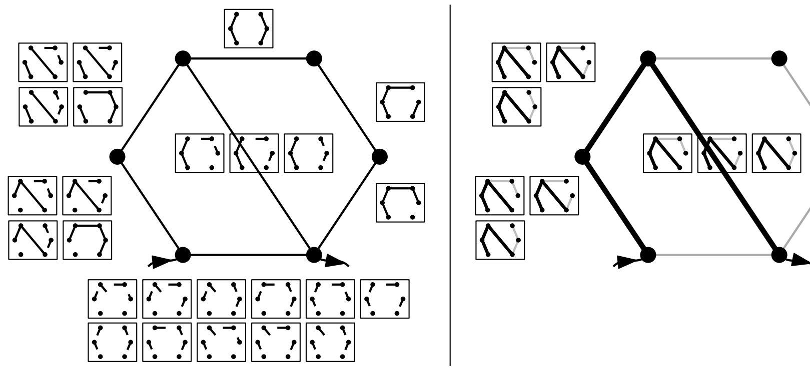

Figure 28: Left: Contributors from trivial classes; Right: The associated spanning trees and unique paths.

Combining Theorem 3.3.1 and Lemma 3.4.1, we can discuss the Cycle and Vertex Conservation properties from Theorem 3.1.2. For a graph there is a natural matching of cancellative contributors within the non-trivial Boolean classes which causes cancellation and produces the conservation laws. The introduction of negative edges may produce non-vanishing Boolean classes as well as matched trivial classes of the same sign.

Lemma 3.4.6 (Contributor Cycle "Conservation") *There is a matching between the elements of*

$$\hat{\mathfrak{C}}^1_{\neq 0}(L^0(G); u_1u_2, w_1w_2) \cup \hat{\mathfrak{C}}^1_{\neq 0}(L^0(G); u_1u_2, w_2w_3) \cup \hat{\mathfrak{C}}^1_{\neq 0}(L^0(G); u_1u_2, w_3w_1).$$

Proof.

Let G be a signed graph with source u_1, sink u_2, and vertices w_1, w_2, and w_3. Additionally, let $e_{w_1w_2}$, $e_{w_2w_3}$, and $e_{w_3w_1}$ be the edges between their respective vertices, or the edge introduced to G if one does not exist.

Consider $c \in \hat{\mathfrak{C}}^1_{\neq 0}(L^0(G); u_1u_2, w_1w_2)$. From Lemma 3.4.1, let P be the unique u_1u_2-path in c made with the inclusion of $e_{w_1w_2}$ so that $P = P_{u_1,w_i} \cup e_{w_1w_2} \cup P_{w_j,u_2}$, where $\{i,j\} = \{1,2\}$. Since c is in a trivial class, there are no circles to activate, and from Corollary 3.4.2 vertex w_3 must be linked to P_{u_1,w_i} or P_{w_j,u_2} by a sequence of unpackings. Moreover, all backsteps outside of circle-activation unpack towards P, so there is a unique vertex w' that meets exactly one of P_{u_1,w_i} or P_{w_j,u_2}.

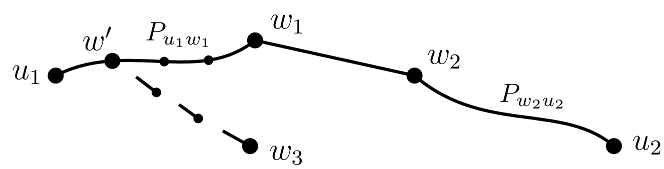

Assume w' meets P_{u_1,w_i}, the case where w' meets P_{w_j,u_2} is similar. Form the path $P' : u_1 \to w' \to w_3$. P' may contain w_i if $w' = w_i$ but cannot contain $e_{w_1w_2}$. Introducing edge e_{w_3,w_j} forms a unique u_1u_2-path $P'' = P' \cup e_{w_3,w_j} \cup P_{w_j,u_2}$ that uses exactly one of $e_{w_1w_2}$, $e_{w_2w_3}$, or $e_{w_3w_1}$. Removing e_{w_3,w_i}, reversing the u_1w_i part of P'', and packing all non-P'' adjacencies away from P'' leaves a unique contributor $c' \in \hat{\mathfrak{C}}^1_{\neq 0}(L^0(G); u_1u_2, w_3w_j)$.

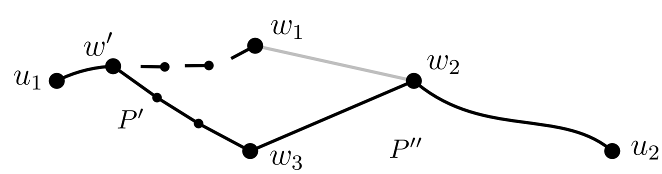

Moreover, there is no corresponding contributor in $\hat{\mathfrak{C}}^1_{\neq 0}(L^0(G); u_1u_2, w_3w_i)$ since e_{w_3,w_i} does not form a path without using more than one of $e_{w_1w_2}$, $e_{w_2w_3}$, and $e_{w_3w_1}$.

■

Tutte's Cycle Conservation in Theorem 3.1.2 comes from Lemma 3.4.6, as every edge is positive and the matching converts between one and two circles, changing their signs. Cancellation of graphs is a specific case of the general rule for signed graphs as opposed to an inherent structural difference between graphs and signed graphs. In general, signed graphic conservation cannot be guaranteed as (1) there may be negative edges between a trivial-class matching, and (2) the non-trivial classes need not cancel. Tutte's Vertex Conservation in Theorem 3.1.2 is also a consequence of the following lemma and is easily seen in Figure 28 by tracing the contributor sorting along source-sink paths.

Lemma 3.4.7 (Vertex "Conservation") *Let G be a signed graph with source u_1, sink u_2, and let v be another vertex.*

1. *If $v \notin \{u_1, u_2\}$, then* $|\bigcup_{x\sim v} \hat{\mathfrak{C}}^1_{\neq 0}(L^0(G); u_1u_2, xv)| = |\bigcup_{y\sim v} \hat{\mathfrak{C}}^1_{\neq 0}(L^0(G); u_1u_2, vy)|$.
2. *If $v \in \{u_1, u_2\}$, then* $|\bigcup_{x\sim v} \hat{\mathfrak{C}}^1_{\neq 0}(L^0(G); u_1u_2, u_1x)| = |\bigcup_{y\sim v} \hat{\mathfrak{C}}^1_{\neq 0}(L^0(G); u_1u_2, yu_2)|$.

Proof.

Let G be a signed graph with source u_1, sink u_2, and let v be another vertex. Consider $\hat{\mathfrak{C}}^1_{\neq 0}(L^0(G); u_1u_2, xv)$ and $\hat{\mathfrak{C}}^1_{\neq 0}(L^0(G); u_1u_2, vy)$, where the edges e_{xv} and e_{vy} exist in G.

Case 1 ($v \notin \{u_1, u_2\}$): If $c \in \hat{\mathfrak{C}}^1_{\neq 0}(L^0(G); u_1u_2, xv)$, using Lemma 3.4.1 consider the u_1u_2-paths that contains e_{xv}. Since v is not the source or sink, each path must contain exactly one of the edges e_{vy} for some y. From Corollary 3.4.2, all contributors in $\hat{\mathfrak{C}}^1_{\neq 0}(L^0(G); u_1u_2, xv)$ associated to a path containing both e_{xv} and e_{vy} must also have a corresponding element in $\hat{\mathfrak{C}}^1(L^0(G); u_1u_2, vy)$.

The argument is identical on the preceding edge when starting with $\hat{\mathfrak{C}}^1(L^0(G); u_1u_2, vy)$.

Case 2 ($v \in \{u_1, u_2\}$): If v is the source, there are no v-entrant edges in any u_1u_2-path. While, if v is the sink, there are no v-salient edges in any u_1u_2-path. However, from Lemma 3.4.1 and Corollary 3.4.2, all contributors arise from u_1u_2-paths, therefore all trivial class contributors out of u_1 have a corresponding contributor in to u_2. ■

Clearly, if every edge of a signed graph is positive, the non-trivial activation classes sum to zero. The trivial classes in each matching above also cancel. Thus, conservation is guaranteed when G has all positive edges.

Corollary 3.4.8 *If G has all positive edges, then the D-contributor-transpedances are both cycle and vertex conservative.*

It is clear, based on an earlier observation, that a graph with a single negative edge that is between the source and sink is conservative, as that edge never appears in any contributor.

4 MAXIMIZING TRANSPEDANCES VIA PERMANENTS

In this section, we will discuss counting total contributors and how permanents, contributors, and the the signless Laplacian can be used to maximize transpedances.

4.1 Contributor Counting

In previous sections, we observed how contributors can be used in determining the characteristic and total minor polynomials [6, 12] and generalizations of the Matrix-tree Theorem [20]. Next, we will examine the net placement of contributors on a graph. This will utilize the fact that the permanent of the oriented hypergraphic signless Laplacian was shown to count the number of contributors, which occurs when every adjacency is negative.

Theorem 4.1.1 ([6], Theorem 4.3.1 part 1) *Let G be an oriented hypergraph with no isolated vertices or 0-edges with Laplacian matrix $\mathbf{L}_G$, then* $\mathrm{perm}(\mathbf{L}_G) = |\mathfrak{C}(G)|$ *if, and only if, every edge of G is extroverted or introverted.*

The previous theorem is a direct calculation on the Laplacian, as we make use of the coefficient of the total minor polynomial to keep track of the ordered minor placement. The *permanental-sign* of a contributor c is taken from Theorem 2.4.3, where

$$sgn_P(c) = (-1)^{nc(c)+bs(c)}.$$

Thus, the signless Laplacian can be used to count the number of reduced contributors for any oriented hypergraph.

Theorem 4.1.2 *If G is an oriented hypergraph with all negative adjacencies, then*

$$\sum_{c \in \hat{\mathfrak{C}}_{\neq 0}(L^0(G);\mathbf{u},\mathbf{w})} sgn_P(c) = (-1)^{|V|-k} \, |\hat{\mathfrak{C}}_{\neq 0}(L^0(G);\mathbf{u},\mathbf{w})|$$

Proof. Let $k = |U| = |W|$ with U and W totally orderings $\mathbf{u}$ and $\mathbf{w}$. Also let $sgn_P(c) = (-1)^{nc(c)+bs(c)}$ be the permanent signing function. We proceed with an inductive argument:

Case 1 ($k = 0$): Observe that if c is a minimal (identity-clone) contributor, then $nc(c) = 0$ and $bs(c) = |V|$, and the permanent sign of all minimal contributors is $(-1)^{|V|}$. If c' is any contributor that can unpack into another covering contributor c'' containing a new cycle of length ℓ, then we have two cases based on ℓ's parity.

Case 1a (ℓ is even): Unpack ℓ backsteps in c' to form a cycle of length ℓ in c''. Since ℓ is even and all edges are negative, we lose ℓ backsteps and gain 0 negative components. Since $-\ell + 0$ is even, $sgn_P(c') = sgn_P(c'')$.

Case 1b (ℓ is odd): Unpack ℓ backsteps in c' to form a cycle of length ℓ in c''. Since ℓ is odd and all edges are negative, we lose ℓ backsteps and gain 1 negative component. Since $-\ell + 1$ is even, $sgn_P(c') = sgn_P(c'')$.

Thus, all contributors have the same sign as their minimal contributor, and all minimal contributors have the same sign, giving

$$\sum_{c \in \hat{\mathfrak{C}}_{\neq 0}(L^0(G);\mathbf{u},\mathbf{w})} sgn_P(c) = (-1)^{|V|} \, |\hat{\mathfrak{C}}(G)|.$$

Case 2 *($k > 0$):* In a contributor with all negative adjacencies, deleting a negative edge will swap the sign of the component that contained the edge, thus changing $nc(c)$ by one. Deleting a backstep will decrease $bs(c)$ by one, which will flip the permanent sign of the total contributor. Since all contributors in $\hat{\mathfrak{C}}(G)$ have the same permanent signing, the sign alternates with every edge or backstep that is removed. Thus, the permanent counts of reduced contributors must be

$(-1)^{|V|-k}|\hat{\mathfrak{C}}_{\neq 0}(L^0(G);\mathbf{u},\mathbf{w})|$. ■

4.2 Signed Graphs and Maximal Transpedances

We have previously defined contributor transpedances for the determinant and now define a similar contributor transpedance for the permanent. The *P-contributor-transpedance*, to be

$$[u_1u_2, w_1w_2]_P = \sum_{c \in \hat{\mathfrak{C}}_{\neq 0}(L^0(G);u_1u_2,w_1w_2)} sgn_P(c).$$

Corollary 4.2.1 *If G is an oriented hypergraph with all negative adjacencies, then*

$$[u_1u_2, w_1w_2]_P = (-1)^{|V|}\,|\hat{\mathfrak{C}}_{\neq 0}(L^0(G);u_1u_2,w_1w_2)|$$

Proof. From Theorem 4.1.2 the value of $[u_1u_2, w_1w_2]_P$ is equal to

$$(-1)^{|V|-2}\,|\hat{\mathfrak{C}}_{\neq 0}(L^0(G);u_1u_2,w_1w_2)|,$$

and $|V|-2$ and $|V|$ have the same parity. ■

The permanent of a signless Laplacian provides a count on the total number of contributors and thus a maximum value, never actually achievable, for the determinant.

Below, we provide further results regarding a permanent version of Tutte's Transpedance Theorem.

Lemma 4.2.2 (P-Contributor Degeneracy) *Let G be a signed graph with source u_1, sink u_2, and distinct vertices w_1, w_2 and w_3, then*

1. $[u_1u_1, w_1w_2]_P = [u_1u_2, w_1w_1]_P = 0,$

2. $[u_1u_2, w_1w_2]_P = [u_1u_2, w_2w_1]_P = [u_2u_1, w_1w_2]_P,$

3. There is a matching between the elements of

$$\hat{\mathfrak{C}}^1_{\neq 0}(L^0(G); u_1u_2, w_1w_2) \cup \hat{\mathfrak{C}}^1_{\neq 0}(L^0(G); u_1u_2, w_2w_3) \cup \hat{\mathfrak{C}}^1_{\neq 0}(L^0(G); u_1u_2, w_3w_1).$$

4. Let G be a signed graph with source u_1, sink u_2, and let v be another vertex.

(a) If $v \notin \{u_1, u_2\}$, then $|\bigcup_{x\sim v} \hat{\mathfrak{C}}^1_{\neq 0}(G; u_1u_2, xv)| = |\bigcup_{y\sim v} \hat{\mathfrak{C}}^1_{\neq 0}(G; u_1u_2, vy)|$.

(b) If $v \in \{u_1, u_2\}$, then $|\bigcup_{x\sim v} \hat{\mathfrak{C}}^1_{\neq 0}(G; u_1u_2, u_1x)| = |\bigcup_{y\sim v} \hat{\mathfrak{C}}^1_{\neq 0}(G; u_1u_2, yu_2)|$.

Proof. The proofs are identical to the determinant case as they are the same set of objects. The only exception is even circles are not included in any signs. ∎

5 HADAMARD'S CONJECTURE

Hadamard's maximum determinant problem ask for the largest possible determinant for an $n \times n$ $\{\pm 1\}$-matrix. Furthermore, the conjecture states that a Hadamard matrix, a $\{\pm 1\}$-matrix of maximal determinant with mutually orthogonal rows, exists only when $n = 1, 2$ or $n \equiv 0 \mod 4$.

When considering the maximum determinant problem for $\{\pm 1\}$-matrices, it is often translated to the maximum determinant problem of $\{0, +1\}$-matrices. Given a $\{\pm 1\}$-matrix, the problem can be *normalized* by row and column negation to have the entries of the first row and first column be entirely $+1$. For a normalized $\{\pm 1\}$-matrix $\mathbf{H}$, let $\mathbf{H}'$ be the matrix obtained by pivoting on the $\{1,1\}$-entry, and $\mathbf{H}'_{1,1}$ be the $\{1,1\}$-minor of $\mathbf{H}'$. The entries of $\mathbf{H}'_{1,1}$ are either 0 or -2, and factoring out the non-zeroes from each row gives a matrix $\mathbf{H}''_{1,1}$ where

$$|\det(\mathbf{H})| = 2^{n-1}|\det(\mathbf{H}''_{1,1})|.$$

Example 5.0.1 *Consider the $\{\pm 1\}$-matrix of size 4, which is a matrix of maximal determinant for a $\{\pm 1\}$-matrix of size 4×4. The following steps demonstrate how to translate to the maximum determinant problem to a $\{0, 1\}$-matrix maximal determinant problem which is a standard practice.*

$$\begin{bmatrix} -1 & 1 & -1 & 1 \\ -1 & -1 & -1 & -1 \\ -1 & 1 & 1 & -1 \\ 1 & 1 & -1 & -1 \end{bmatrix} \xrightarrow{norm} \begin{bmatrix} 1 & 1 & 1 & 1 \\ 1 & -1 & 1 & -1 \\ 1 & 1 & -1 & -1 \\ 1 & -1 & -1 & 1 \end{bmatrix} \xrightarrow{pivot} \begin{bmatrix} 1 & 1 & 1 & 1 \\ 0 & -2 & 0 & -2 \\ 0 & 0 & -2 & -2 \\ 0 & -2 & -2 & 0 \end{bmatrix}$$

$$\xrightarrow{minor} \begin{bmatrix} -2 & 0 & -2 \\ 0 & -2 & -2 \\ -2 & -2 & 0 \end{bmatrix} \xrightarrow{factor} \begin{bmatrix} 1 & 0 & 1 \\ 0 & 1 & 1 \\ 1 & 1 & 0 \end{bmatrix}.$$

We will instead consider the meaning of the $\{-2, 0\}$ matrix.

This process allows for reinterpretation of Hadamard's maximum determinant problem and allows us to consider the relationship to incidence orientations of hypergraphs. For the following sections we will consider each $n \times n$ $\{\pm 1\}$-matrix to be an incidence matrix for an n-full oriented hypergraph. An *n-full* oriented hypergraph has n vertices and n edges, so that each edge is incident to each vertex.

5.1 Fundamental Bouquet

We want to examine the fundamental components of these matrices. To make the process more streamlined, we begin by noting that for oriented hypergraphs the normalization process is equivalent to vertex- and edge-*switching* in an oriented hypergraph (that is to say, re-orienting the incidences at a vertex or within an edge). Switching does not alter the sign of any circle in an oriented hypergraph [21], so for each associated n-full oriented hypergraph, we may assume that every adjacency through e_1 as well as every co-adjacency through v_1, is negative. Each $\{k, \ell\}$-entry of the associated $\{0, +1\}$-matrix is naturally associated to the 2×2 minors of $\mathbf{H}$ of the form

$$\begin{bmatrix} h_{1,1} & h_{1,\ell} \\ h_{k,1} & h_{k,\ell} \end{bmatrix}.$$

These minors also correspond to digons in G that contain v_1 and e_1 and are called the *fundamental bouquet* of G. Example 5.1.1 depicts the digons in G that correspond to the entries highlighted in Example 5.0.1 matched by color.

Example 5.1.1 *Figure 29 (left) depicts the associated oriented hypergraph G to the normalized matrix. H in Example 5.0.1. Observe that all the incidences in e_1 and at v_1 are vertex-entrant (+1).*

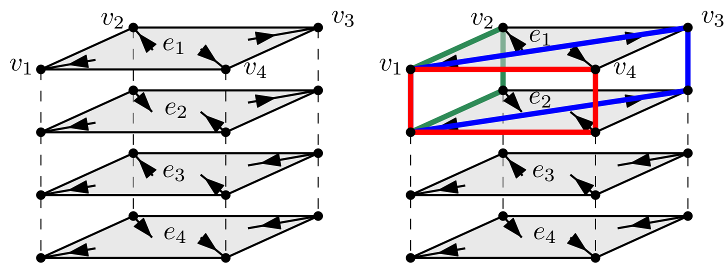

Figure 29: An example of an n-full oriented hypergraph with digons. Left: A normalized n-full oriented hypergraph G; Right: The 0 and +1 entries in the reduction of a normalized $\{-1,+1\}$-matrix correspond to positive and negative digons in G.

Figure 29 (right) depicts digons of the fundamental bouquet between edges e_1 and e_2 in Example 5.0.1.

Lemma 5.1.2 *The fundamental bouquet of an n-full oriented hypergraph is a set of fundamental circles. Moreover, a digon is positive (negative) if and only if the corresponding entry in the associated $\{0,+1\}$-matrix is 0 $(+1)$.*

Proof. There are $(n-1)^2$ entries in the $\{1,1\}$-minor that correspond to the digons in the fundamental bouquet. From [21] the cyclomatic number is calculated on the bipartite incidence graph of an incidence hypergraph, so the cyclomatic number of an n-full oriented hypergraph is

$$\phi(G) = |I| - (|V| + |E|) + 1 = (n-1)^2.$$

Thus, there are $(n-1)^2$ incidences whose deletion results in a circle-free incidence hypergraph. Specifically, each incidence corresponding to entry $h_{k,\ell}$ may be deleted.

A digon sign property is immediate from the fact that the determinant of a positive circle is 0 and a negative circle is ±2. ∎

From here, we see that the entries that are +1 in the equivalent $\{0, +1\}$-matrix are negative digons in G that contain v_1 and e_1 that, ideally, all appear in a permutation in the $\{0, +1\}$-matrix. This gives an immediate re-interpretation of the maximum determinant problem. From here, the next step is to characterize the orientations of an n-full incidence hypergraph in terms of negative digon placement in a fundamental bouquet that maximizes the determinant.

5.2 Fundamental Necklace

From Section 5.1, we modify the fundamental bouquets into strands of consecutive digons using vertex- and edge-thetas and Lemma 2.1.6. A *strand* of digons of the form $(v_k, e_1, v_{k+1}, e_2, v_k)$ for $k \in \{1, 2, \ldots, n-1\}$ is made from a fundamental bouquet by taking the edge-thetas between e_1, e_2 with co-adjacencies (e_1, v_1, e_2), (e_1, v_k, e_2), and (e_1, v_{k+1}, e_2). There is an immediate dual formulation using vertex-thetas that moves to a new consecutive edge pair $e_\ell, e_{\ell+1}$. By applying the edge-theta construction between these new edges, we form another strand of digons and let the collections of these digons be the *fundamental necklace* of digons.

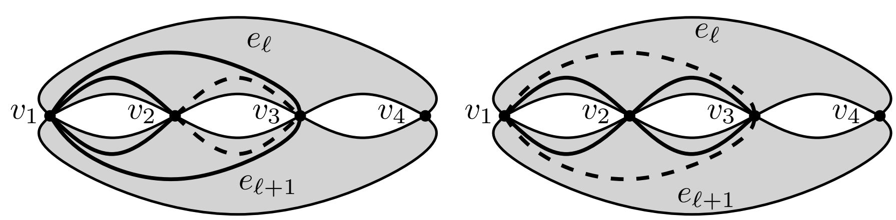

Figure 30: Transitioning between the fundamental bouquet and necklace. Left: Two digons in a fundamental bouquet (solid) and the third digon (dashed) in its edge-theta; Right: Exchange a bouquet digon to add another consecutive digon to a strand in the fundamental necklace.

The digons of a fundamental necklace are the 2×2 minors of the form

$$\begin{bmatrix} h_{k,\ell} & h_{k,\ell+1} \\ h_{k+1,\ell} & h_{k+1,\ell+1} \end{bmatrix}$$

where the determinant is ±2 if and only if the digon is negative (and 0 when positive).

This theta-exchange property takes digons that contribute to the determinant of the equivalent $\{0, +1\}$-matrix to digons that provide insight on orthogonality.

Lemma 5.2.1 *Every digon in the strand between e_k and e_l is negative whenever their corresponding columns are orthogonal.*

Proof. Two $\{-1, +1\}$-vectors are orthogonal if their entries agree exactly half of the time. Thus, each associated digon has three incidences oriented the same and one that is not, forcing the digon to be negative. ■

Clearly if every digon in a strand is negative, the corresponding columns (rows) need not be orthogonal — this is easily checked on 3-edges. However, using the edge- and vertex-thetas as before, the necklace signs can be translated back to the fundamental bouquet to produce the entries of the $\{0, +1\}$-minor. Thus, the fundamental bouquet directly addresses the placement of entries in the $\{0, +1\}$-minor, while the fundamental necklace addresses orthogonality. A characterization of this relationship would indicate how orthogonality interacts with the maximal determinant.

5.3 Tail-Equivalence Classes of n-full Hypergraphs

In this section, we discuss specific observations about tail-equivalence classes of oriented hypergraphs. We begin by adding the following observations to those that we made in Section 3.2. The number of contributors on a single k-edge follow the Stirling numbers of the first kind. For an n-full hypergraph, there are $n!$ elements in each tail-equivalence class (one for each permutation) and n^n different contributors that correspond to the identity permutation (one for each contributor that consists of only backsteps). Note that many contributors may correspond to the same permutation, but must lie in different tail-equivalence classes.

Example 5.3.1 *Given a 3-full incidence hypergraph (left) consider the identity-contributor consisting of* 3 *backsteps in Figure 31 (right).*

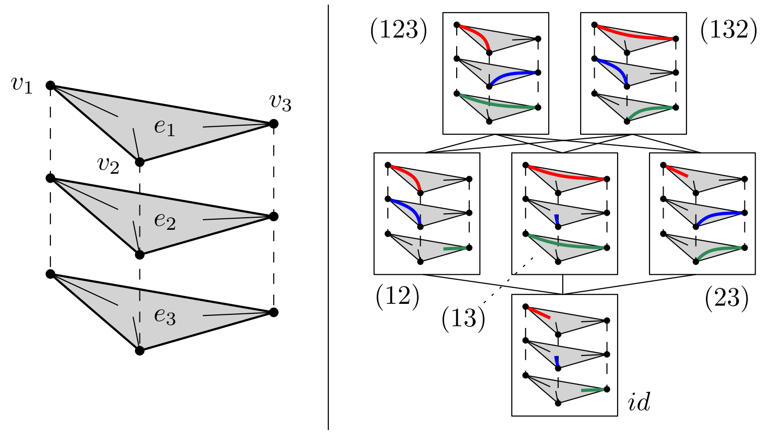

Figure 31: A 3-full incidence hypergraph (right) and one of its tail-equivalence classes (left).

This example harkens back to the initial definition and commentary on equivalence classes provided in Section 3.2 where we discuss the distinct permutations and number of contributors in each tail-equivalence class. Each backstep can be individually extended to a sequence of adjacencies that form new permutations. These adjacencies occur within the edge determined by the tail-incidence of each backstep. The entire tail-equivalence class is in Figure 31 (right).

There is an obvious way to separate these classes into two types: (1) the *edge-monic* case where the image of each tail-incidence resides in a different edge, and (2) the non-edge-monic case where two tail-incidences reside in a common edge. Observe that the identity-contributor in Figure 31 is edge-monic.

Let $\mathfrak{A}$ denote the set of tail-equivalence classes, let $\mathfrak{A}_1$ be the set of edge-monic tail-equivalence classes, and let $\mathfrak{A}_2$ be the set of non-edge-monic tail-equivalence classes. We now show that the non-edge-monic tail-equivalence classes cancel over any orientation of an n-full incidence hypergraph.

Theorem 5.3.2 *For an n-full oriented hypergraph G, the sum of the non-edge-monic contributors is zero regardless of orientation, and*

$$\det(\mathbf{L}_G) = \sum_{\mathcal{A}\in\mathfrak{A}_1}\sum_{c\in\mathcal{A}}(-1)^{pc(c)}.$$

Proof. From part 2 of Theorem 2.4.1 we sum the contributors over their activation classes:

$$\begin{aligned}\det(\mathbf{L}_G) &= \sum_{c\in\mathfrak{C}(G)}(-1)^{pc(c)} = \sum_{\mathcal{A}\in\mathfrak{A}}\sum_{c\in\mathcal{A}}(-1)^{pc(c)}\\ &= \sum_{\mathcal{A}\in\mathfrak{A}_1}\sum_{c\in\mathcal{A}}(-1)^{pc(c)} + \sum_{\mathcal{A}\in\mathfrak{A}_2}\sum_{c\in\mathcal{A}}(-1)^{pc(c)},\end{aligned}$$

and we show that the second sum is zero. Specifically, for any $\mathcal{A}\in\mathfrak{A}_2$

$$\sum_{c\in\mathcal{A}}(-1)^{pc(c)} = 0.$$

Let $\mathcal{A}\in\mathfrak{A}_2$, since $\mathcal{A}$ is a non-edge-monic tail-equivalence class, there exist distinct vertices v and w such that $c(e_v) = c(e_w)$ for every contributor c. Let the permutation $\pi' = \pi\cdot(vw)$ be the permutation obtained by multiplying by the transposition (vw); clearly, $(\pi')' = \pi$. Also, since each tail-equivalence class contains every permutation, let c_π be the contributor of $\mathcal{A}$ corresponding to permutation π.

Since $\mathcal{A}$ is a tail-equivalence class the set of tail-incidences of c_π and $c_{\pi'}$ are identical. Let the head maps $c_\pi(h_v) = a$ and $c_\pi(h_w) = b$, then we see that $c_{\pi'}(h_v) = b$ and $c_{\pi'}(h_w) = a$. Moreover, their respective head-incidences of v and w belong to the same edge so c_π and $c_{\pi'}$ also have the same head-incidences. Thus, the incidences of c_π and $c_{\pi'}$ are identical.

Case 1: One of c_π or $c_{\pi'}$ has v and w in a disjoint 2-cycle using the same adjacency twice, and the other has a backstep at v and w within the same edge. In this case c_π and $c_{\pi'}$ differ by a single positive circle.

Case 2: Neither c_π and $c_{\pi'}$ have v and w in a disjoint 2-cycle using the same adjacency twice. In this case c_π and $c_{\pi'}$ have the same set of incidences but differ by a single adjacency. Thus, they differ by a sign.

Summing over all the contributors of $\mathcal{A}$ we get

$$2\sum_{c\in\mathcal{A}}(-1)^{pc(c)} = \sum_{\pi}\left[(-1)^{pc(c_\pi)} + (-1)^{pc(c_{\pi'})}\right] = 0,$$

and

$$\sum_{\mathcal{A}\in\mathfrak{A}_1}\sum_{c\in\mathcal{A}}(-1)^{pc(c)} + \sum_{\mathcal{A}\in\mathfrak{A}_2}\sum_{c\in\mathcal{A}}(-1)^{pc(c)} = \sum_{\mathcal{A}\in\mathfrak{A}_1}\sum_{c\in\mathcal{A}}(-1)^{pc(c)}.$$

■

As a result of Theorem 5.3.2, we can turn our attention to the main theorem on edge-monic contributors. Recall that $\mathfrak{A}_1$ is the set of edge-monic tail-equivalence classes.

Theorem 5.3.3 *Let G be an n-full oriented hypergraph. If $\mathcal{A}\in\mathfrak{A}_1$, then*

$$\left|\sum_{c\in\mathcal{A}}(-1)^{pc(c)}\right| = |\det(\mathbf{H}_G)|.$$

Proof. We begin by converting the positive circle count $pc(c)$ into a negative circle count as follows:

$$\sum_{c\in\mathcal{A}}(-1)^{pc(c)} = \sum_{c\in\mathcal{A}}(-1)^{tc(c)+nc(c)},$$

where $nc(c)$ is the number of negative circles of c, and $tc(c)$ is the total number of circles in c. Given that the sum is a power for -1, we can add the negative circle count as opposed to subtracting it.

Now, partition the total circle count into even circles $ec(c)$ and odd circles $oc(c)$ giving

$$\sum_{c \in \mathcal{A}} (-1)^{tc(c)+nc(c)} = \sum_{c \in \mathcal{A}} (-1)^{ec(c)+oc(c)+nc(c)}.$$

However,

$$\sum_{c \in \mathcal{A}} (-1)^{ec(c)+oc(c)+nc(c)} = \sum_{c \in \mathcal{A}} (-1)^{ec(c)} \prod_{v \in V} \sigma(c(i_v))\sigma(c(j_v)).$$

This last equality is because every contributor corresponds to a permutation, and the value $\sigma(c(i_v))\sigma(c(j_v))$ is the adjacency/backstep entry of $\mathbf{L}_G$ [6]. Since $\mathbf{L}_G = \mathbf{D}_G - \mathbf{A}_G$ [17] the parity equivalence is seen by factoring out a -1 for each adjacency to get $(-1)^{oc(c)}$, and factoring out a -1 for each negative adjacency to get $(-1)^{nc(c)}$.

Taking the absolute value and separating the product gives

$$\left| \sum_{c \in \mathcal{A}} (-1)^{pc(c)} \right| = \left| \sum_{c \in \mathcal{A}} (-1)^{ec(c)} \prod_{v \in V} \sigma(c(i_v)) \prod_{v \in V} \sigma(c(j_v)) \right|.$$

However, since $\mathcal{A}$ is a tail-equivalence class, the tail product term

$$\prod_{v \in V} \sigma(c(i_v))$$

is the same for each contributor and has magnitude 1. Thus,

$$\left| \sum_{c \in \mathcal{A}} (-1)^{pc(c)} \right| = \left| \sum_{c \in \mathcal{A}} (-1)^{ec(c)} \prod_{v \in V} \sigma(c(j_v)) \right|.$$

This last term is $\det(\mathbf{H}_G)$ since every permutation is represented in an n-full activation class, $(-1)^{ec(c)}$ is the sign of the corresponding permutation, and $\sigma(c(j_v))$

is the entry in the incidence matrix. ■

Thus, any edge-monic class can be used to examine the maximum determinant problem; therefore, determining an orientation that minimizes cancellation on a fixed edge-monic tail-equivalence class is sufficient.

Example 5.3.4 *Figure 32 below depicts a single edge-monic tail-equivalence class with backsteps at each v_i, e_i. The vertices in the tail-equivalence class have v_1 at the top and v_4 at the bottom.*

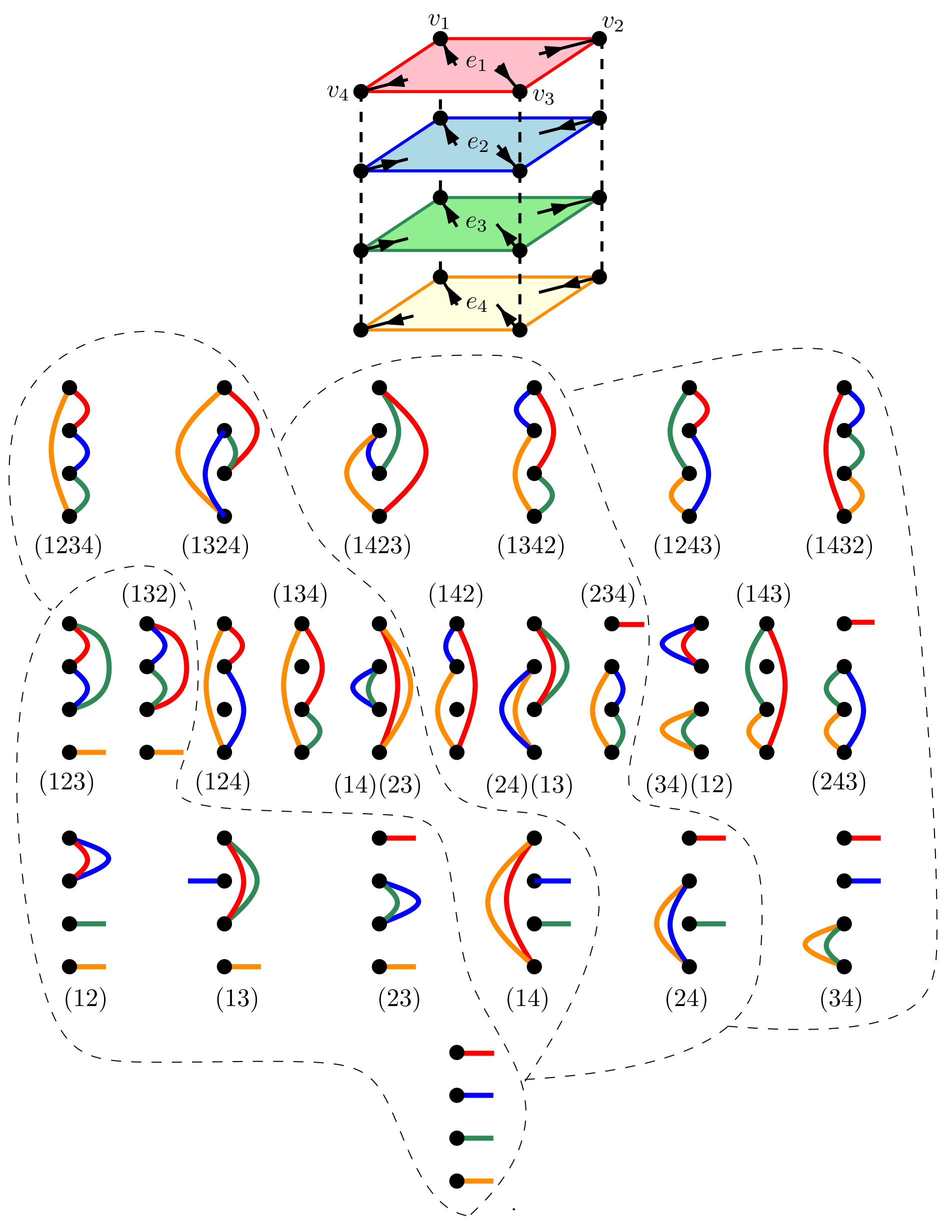

Figure 32: The contributor poset for an 4-full oriented hypergraph

The dashed regions each contain a poset matching those of the 3*-full oriented hypergraph case. The region containing the identity contributor is exactly a tail-equivalence class from the* $n = 3$ *case with* v_4 *in* e_4 *as a backstep. In each of the other regions, the new vertex,* v_4*, is paired with one of the other vertices. The containment of the prior case is interesting, but we cannot simply build cases directly from the previous one as shown by Theorem 1.0.1.*

The maximization of this signed tail-equivalence class can be used to maximize the entire $\{\pm 1\}$*-matrix. The incidence orientations of the* 4*-full oriented hypergraph represent an incidence matrix with maximum determinant. The backsteps are sequentially unpacked to provide contributors whose sign pattern is:*

$$\begin{array}{c}
+ \quad + \quad + \quad - \quad - \quad + \\[1em]
+ \quad + \quad + \quad + \quad + \quad + \quad + \quad + \quad + \quad + \quad + \\[1em]
+ \quad + \quad - \quad - \quad + \quad + \\[1em]
+
\end{array}$$

The determinant is $20 - 4 = 16$*, as there are* 24 *contributors,* 20 *of which are positive and* 4 *of which are negative. This is the fewest number of negative contributors possible, hence the determinant is maximal.*

5.4 Symmetries and Additional Structure

Given Theorem 5.3.3, an individual edge-monic tail-equivalence class may be used to study the maximum determinant problem. It seems we only need to consider a single class, and the rest are irrelevant. However, there are nice symmetries between these classes. We investigate some of these symmetry results to help contextualize the maximum determinant contributor relationships as well as provide other potentially helpful avenues by which to address the problem.

5.4.1 Edge-monic Class Comparison

In this section, we want to illustrate the relationship between edge-monic class orientations, sums, and the determinant. For an n-full incidence hypergraph G with orientation σ, let P_σ (respectively N_σ) be the number of edge-monic tail-equivalence classes that sum to a positive (respectively negative) number given the orientation σ.

Lemma 5.4.1 *The maximum determinant problem is equivalent to* $\max_\sigma(P_\sigma - N_\sigma)$*, over all incidence orientations* σ*.*

Proof. By Theorem 5.3.2, summing over all the contributors in all edge-monic tail-equivalence classes gives the determinant of the Laplacian $\det(\mathbf{H}_G)^2$, so we may assume $P_\sigma \geq N_\sigma$. From Theorem 5.3.3 the sum of a given edge-monic tail-equivalence class is the determinant of the incidence matrix up to sign. Summing over all edge-monic tail-equivalence classes that are positive and negative gives

$$\det(\mathbf{H}_G)P_\sigma - \det(\mathbf{H}_G)N_\sigma = \det(\mathbf{H}_G)^2, \text{ and}$$
$$P_\sigma - N_\sigma = \det(\mathbf{H}_G).$$

■

Thus, we can either use a single edge-monic class and maximize positive contributors, or we can use all the classes and maximize those that sum to a positive number. One of these may turn out to be an easier process than the other. From Lemma 5.4.1 we can immediately see the following corollary.

Corollary 5.4.2 *If G be an n-full oriented hypergraph with orientation σ, then*

$$\det(\mathbf{H}_G) = n! - 2N_\sigma$$

$$\det(\mathbf{H}_G) = 2P_\sigma - n!$$

assuming $P_\sigma \geq N_\sigma$.

Proof. Use Lemma 5.4.1, and the fact that there are $n!$ edge-monic tail-equivalence classes so $P_\sigma + N_\sigma = n!$. ■

Example 5.4.3 *In Figure 33, we see the six edge-monic tail-equivalence classes for the $n = 3$ Hadamard case. They all sum to ± 4 in the maximal determinant case.*

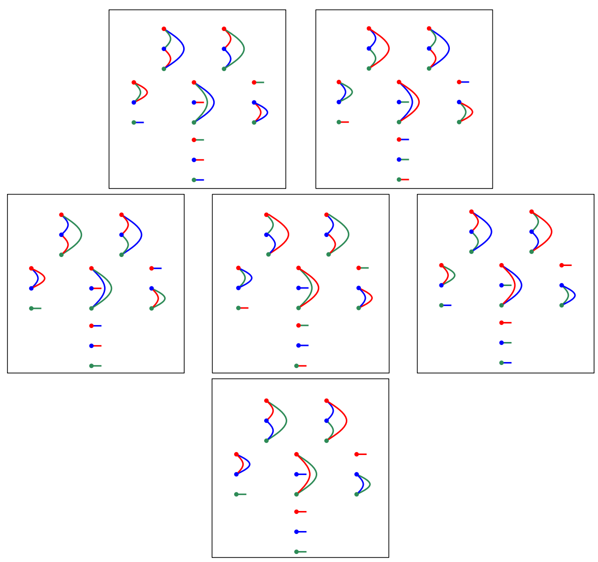

Figure 33: Poset of posets for 3-full Oriented Hypergraph

Using Lemma 5.4.1, we see that $det(L) = 4^2 = 16$. Given that we have six edge-monic classes, we can determine that there are five edge-monic classes summing to $+4$ and one edge-monic tail-equivalence class summing to -4. By Corollary 5.4.2, we see that $det(\mathbf{H}_G) = n! - 2N_\sigma = 3! - 2(1) = 6 - 2 = 4$. While this holds for all determinants, the problem is now determining the smallest value for N_σ.

Given what we have seen in this section, the next step is to determine the relationship of the number of positive (or negative) edge-monic tail-equivalence classes to a given orientation.

5.4.2 Adjacency Equivalence

In this section, we will begin the discussion of the relationship between contributors with similar adjacency structures in different edge-monic tail-equivalence classes. An n-full incidence hypergraph has n vertices and n edges. Thus, the tail-incidence of each edge-monic tail-equivalence class can be considered to be an intermediary permutation between the vertex and edge sets. We do this via a lexicographic order obtained from the incidence matrix. This allows for each edge-monic tail-equivalence class to have a unique permutation $k \mapsto \ell$ for $k, \ell \in \{1, 2, \ldots, n\}$ associated to each tail-incidence with ends v_k and e_ℓ. For each $\mathcal{A} \in \mathfrak{A}_1$ call this intermediary permutation the *identifier* of $\mathcal{A}$. Let $\mathcal{A}_\alpha$ denote the edge-monic tail-equivalence class with identifier α.

Example 5.4.4 *Here we see two tail-equivalence classes and their identifiers. The two classes are* $\mathcal{A}_{id}$ *and* $\mathcal{A}_{(123)}$.

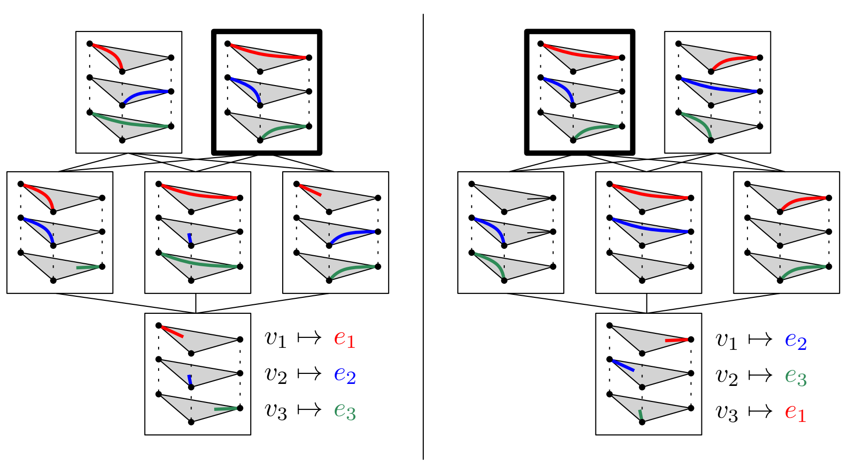

Figure 34: Two tail-equivalence classes $\mathcal{A}_{id}$ (left) and $\mathcal{A}_{(123)}$ (right) as determined by $v_k \mapsto e_\ell$.

Looking at the two contributors in the bolded boxes, we see that they initially appear to be the same. However, we can see from the identifier that the head and tails of the adjacencies are reversed.

Consider two different identifiers α and β; there is exactly one such element in each of $\mathcal{A}_\alpha$ and $\mathcal{A}_\beta$ where the head and tail incidences are reversed. These are determined by the composition

$$V \xrightarrow{\alpha} E \xrightarrow{\beta^{-1}} V \ ,$$

and its inverse. These contributors are said to be *adjacency-equivalent*, and obviously have the same sign. In Figure 34, the contributors $c_{(132)} \in \mathcal{A}_{id}$ and $c_{(123)} \in \mathcal{A}_{(123)}$ (bolded boxed) are the adjacency-equivalent pair.

Lemma 5.4.5 *Given any $\mathcal{A}_\alpha$ and $\mathcal{A}_\beta$ in $\mathfrak{A}_1$, there is a exactly one adjacency-equivalent pair of contributors. These contributors are $c_{\alpha^{-1}\beta} \in \mathcal{A}_\beta$ and $c_{\beta^{-1}\alpha} \in \mathcal{A}_\alpha$. Moreover, these elements are orientation reversals.*

Since the signs remain the same across classes, this alludes to a possible technique to understand the relationship between the number of positive and negative edge-monic tail-equivalence classes in a given orientation.

Corollary 5.4.6 *The set of contributors that are adjacency-equivalent to the elements of $\mathcal{A}_\alpha$, along with $c_{id} \in \mathcal{A}_\alpha$, is a transversal of all edge-monic tail-equivalence classes. Moreover, these transversals form a disjoint covering of all edge-monic contributors.*

Example 5.4.7 *In this figure, we see how the contributors from different edge-monic tail-equivalence classes relate to each other.*

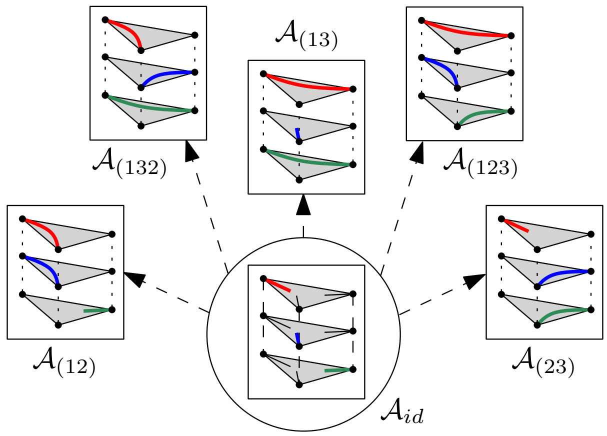

Figure 35: The elements of $\mathcal{A}_{id}$ produce a transversal of the edge-monic classes via adjacency-equivalence.

This relationship highlights how maximizing a single edge-monic tail-equivalence class will maximize the entire problem.

5.4.3 A Fundamental Set in Edge-monic Classes

In this section, we address how to build a fundamental set of cycles to minimize the number of contributor signs that must be examined in order to maximize the determinant. Notice there are only $\binom{n}{2}$ digons in each tail-equivalence class, which is not sufficient for a fundamental set. So, we produce a new set of fundamental circles for the edge-monic tail-equivalence classes. We begin by defining specific path configurations. A *k-cross-theta* consists of k internally-disjoint paths between a vertex and an edge. Let G be an n-full oriented hypergraph and $\mathcal{A}_\alpha \in \mathfrak{A}_1$. For each k, $1 \leq k \leq n$, create the following sequence of $(n-k+1)$-cross-thetas; let Θ_1 be the n-cross-theta between v_1 and $e_{\alpha(1)}$, and define subsequent Θ_k as the $(n-k+1)$-cross-theta between v_k and $e_{\alpha(k)}$ avoiding the previous vertices and edges. This is called a *k-cross-theta decomposition* of $\mathcal{A}_\alpha \in \mathfrak{A}_1$.

For Θ_1 out of v_1, the adjacency steps all use the same tail-incidence to $e_{\alpha(1)}$

before ending as some v_k. Moreover, all returning adjacencies belong to a different edge, so their non-v_1-end must be the tail-end of v_k. Thus, an n-cross-theta constructed out of a single initial vertex determines the identifier. The $\binom{n}{2}$ digons in a k-cross-theta decomposition are precisely the contributors in $\mathcal{A}_\alpha$ containing a single digon (corresponding to a single transposition). The below figure illustrates how a k-cross-theta appears between the edges.

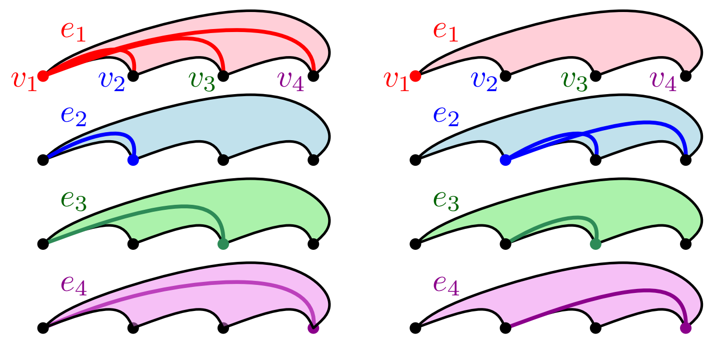

Figure 36: Θ_1 and Θ_2 for a 4-full hypergraph of $\mathcal{A}_{id}$.

Now that we have defined how digons and k-cross-thetas appear in the graph, let us examine their appearance within a matrix. These digons correspond to the 2×2 minors of the form

$$\begin{bmatrix} h_{k,k} & h_{k,\ell} \\ h_{\ell,k} & h_{\ell,\ell} \end{bmatrix},$$

and, for the 4-full example in Figure 36, the incidence matrix entries appearing in Θ_1 and Θ_2 are depicted as solid circles.

$$\underset{\Theta_1}{\begin{bmatrix} \bullet & \bullet & \bullet & \bullet \\ \bullet & \bullet & \cdot & \cdot \\ \bullet & \cdot & \bullet & \cdot \\ \bullet & \cdot & \cdot & \bullet \end{bmatrix}} \qquad \underset{\Theta_2}{\begin{bmatrix} \varnothing & \varnothing & \varnothing & \varnothing \\ \varnothing & \bullet & \bullet & \bullet \\ \varnothing & \bullet & \bullet & \cdot \\ \varnothing & \bullet & \cdot & \bullet \end{bmatrix}}.$$

While there are not enough digons in $\mathcal{A}_\alpha$ to form a fundamental set of circles, the inclusion of a subset of 3-circle contributors not only produces a fundamental set of circles, but the entries of the original incidence matrix $\mathbf{H}_G$ can be calculated using only the signs of these contributors. This means that understanding how the signs of contributors impact the other contributors can allow us to maximize the sum of all contributors through maximizing just this fundamental set. In Theorem 5.4.8, we will see how these contributors determine the matrix entries.

Through normalization, we may assume the incidence matrices have a value of +1 for the first row and column, and by Theorem 5.3.3, we may assume we are working with $\mathcal{A}_{id}$. To simplify the discussion, define the *sign of contributor* c to be $\operatorname{sgn}(c) = (-1)^{pc(c)}$.

Theorem 5.4.8 *The digons in the* Θ_k *and the* 3*-circles with corresponding permutation* $(1k\ell)$ *with* $1 < k < \ell$ *form a fundamental set of circles. Moreover, the entries of the incidence matrix are:*

1. $h_{k,k} = -\operatorname{sgn}(c_{(1k)})$,

2. $h_{k,\ell} = \operatorname{sgn}(c_{(1k\ell)}) \cdot \operatorname{sgn}(c_{(1k)}) \cdot \operatorname{sgn}(c_{(1\ell)})$,

3. $h_{\ell,k} = -\operatorname{sgn}(c_{(1k\ell)}) \cdot \operatorname{sgn}(c_{(k\ell)})$.

Proof. Clearly, from the Stirling numbers of the first kind, there are $s(n, n-1) + s(n-1, n-2) = (n-1)^2$ permutations in this set. We now demonstrate that the remaining entries of a normalized matrix can be determined using only these permutations, and the sign of their associated contributor.

Assume G is normalized so that the all $h_{1,k} = h_{k,1} = +1$, and by Theorem 5.3.3 assume we are working with $\mathcal{A}_{id}$. There is exactly one free entry (incidence) in each digon of Θ_1 which corresponds to $h_{k,k}$, $k \geq 2$. The product of the incidences (entries) for these digons are

$$h_{1,1} \cdot h_{1,k} \cdot h_{k,k} \cdot h_{k,1} = h_{k,k}. \tag{5.4.1}$$

The digons in the Θ_k $(1 < k \leq \ell)$ correspond to the contributors $c_{(k\ell)}$, and have incidence (entry) product

$$h_{k,k} \cdot h_{k,\ell} \cdot h_{\ell,k} \cdot h_{\ell,\ell}. \tag{5.4.2}$$

While the 3-cycle in $c_{(1k\ell)}$ has the following incidence product

$$h_{1,1} \cdot h_{1,k} \cdot h_{k,k} \cdot h_{k,\ell} \cdot h_{\ell,\ell} \cdot h_{\ell,1} = h_{k,k} \cdot h_{k,\ell} \cdot h_{\ell,\ell}. \tag{5.4.3}$$

The main diagonal is set by Equation 5.4.1. Once the main diagonal is set the entries above the diagonal are set by Equation 5.4.3, and then the entries below the diagonal are set by Equation 5.4.2. Thus, we only need to determine the contributor signs of all the digons and $c_{(1k\ell)}$, and the remaining contributor signs depend on these.

Recall that $\operatorname{sgn}(c) = (-1)^{pc(c)}$, and observe that if c_π contains a single cycle of sign ϵ, then $\operatorname{sgn}(c_\pi) = -\epsilon$. Thus, if $h_{k,k} = +1$ the digon in $c_{(1k)}$ is positive, and $\operatorname{sgn}(c_{(1k)}) = -1$; if $h_{k,k} = -1$ the digon in $c_{(1k)}$ is negative, and $\operatorname{sgn}(c_{(1k)}) = +1$; giving $\operatorname{sgn}(c_{(1k)}) = -h_{k,k}$. The 3-cycle in $c_{(1k\ell)}$ has its circle sign equal to the product of the incidences in Equation 5.4.2 and $(-1)^3$, as there are 3 adjacencies. Using $\operatorname{sgn}(c_{(1k)}) = -h_{k,k}$ this reduces to $\operatorname{sgn}(c_{(1k\ell)}) = h_{k,\ell} \cdot \operatorname{sgn}(c_{(1k)}) \cdot \operatorname{sgn}(c_{(1\ell)})$. Finally, the digons in the Θ_k correspond to $c_{(k\ell)}$, which contains a single cycle. The same argument gives $\operatorname{sgn}(c_{(k\ell)}) = -\operatorname{sgn}(c_{(1k\ell)}) \cdot h_{\ell,k}$. Solving for each h entry completes the proof.

■

Next, we want to consider how 3-circles and digons relate to the tail-equivalence classes. Consider a contributor of the form $c_{(1k\ell)} \in \mathcal{A}_{id}$, where $k < \ell$. There is a natural 3-cross-theta formed where two of the three circles belong to the same edge-monic tail-equivalence class. Specifically, $c_{(1k)}, c_{(1k\ell)} \in \mathcal{A}_{id}$ and $c_{(k\ell)} \notin \mathcal{A}_{id}$.

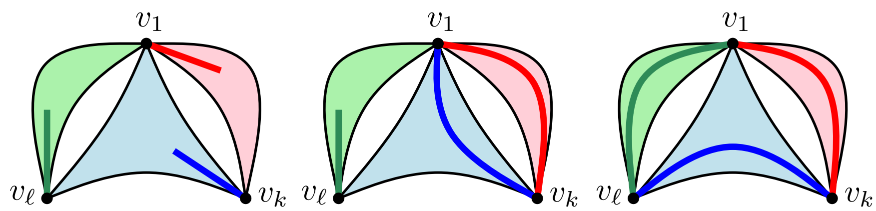

Figure 37: The 3-circle in a 3-cross-theta (right) and one of its digons (center) are in the same class (left).

We can sign these via Lemma 2.1.6, and the digon **not** in $\mathcal{A}_{id}$ determines the sign of $c_{(1k\ell)}$. This observation and Corollary 5.4.6 examine how signs transfer between edge-monic classes. Additionally, the digon of a given cross-theta that leaves the edge-monic class may belong to a fundamental bouquet or necklace. These are all sets of fundamental circles related by different theta configurations. This may yield enough structure to eventually provide a new closed formula for the maximum determinant problem. In order to do this, we need to characterize how cross-theta signs relate across the edge-monic tail-equivalence classes and how they interact with fundamental bouquets and necklaces.

5.4.4 Adjacency Complement

In this section, we want to further examine the relationship between a set of three digons using three specified adjacencies and the two associated contributors using those same adjacencies in circles. Take three digon-contributors $c_{(ab)}$, $c_{(bc)}$, and $c_{(ac)}$ in $\mathcal{A}_\alpha \in \mathfrak{A}_1$ and the two unique contributors $c_{(abc)}$ and $c_{(acb)}$ that use only the adjacencies of the digons. The contributors $c_{(abc)}$ and $c_{(acb)}$ are said to be *adjacency complements* in $\mathcal{A}_\alpha$ with respect to $c_{(ab)}$, $c_{(bc)}$, and $c_{(ac)}$. Clearly,

$$\operatorname{sgn}(c_{(ab)})\operatorname{sgn}(c_{(bc)})\operatorname{sgn}(c_{(ac)}) = -\operatorname{sgn}(c_{(abc)})\operatorname{sgn}(c_{(acb)}), \tag{5.4.4}$$

and this technique can easily be extended to longer permutations, but is not done here.

Example 5.4.9 *The three digons in Figure 31 have the two* 3*-circles above them as adjacency complements. The* 3×3 *matrix below, the incidence matrix with the maximal determinant, has all the digons negative (hence the sign* $(-1)^{pc(c)}$ *is positive),*

$$\begin{bmatrix} 1 & 1 & 1 \\ 1 & -1 & 1 \\ 1 & 1 & -1 \end{bmatrix}.$$

By Equation 5.4.4, the two 3*-circles must have opposite signs. Thus, there are* 5 *positive contributors and one negative in the tail-equivalence class. Since the determinant is the sum of these, we know the determinant is* ± 4*. This is a way to get the determinant value that differs from the method examined in Example 5.4.3.*

It would be ideal if we could assume that all digon-contributors for a specified identity have the same sign. This is not possible due to a sign trade-off between the fundamental 3-circles of the form $(1k\ell)$ and the digons. We can see this issue in the following two matrices.

Consider the 5×5 matrix below whose determinant is maximal:

$$\begin{bmatrix} 1 & 1 & 1 & 1 & 1 \\ 1 & 1 & -1 & -1 & 1 \\ 1 & -1 & 1 & -1 & 1 \\ 1 & -1 & -1 & 1 & -1 \\ 1 & 1 & 1 & -1 & -1 \end{bmatrix}.$$

The only identifier in which all the digon-contributors are negative is $\alpha = (14)(23)$ and there are none where they are all positive. The 6×6 matrix below also has a maximal determinant,

$$\begin{bmatrix} 1 & 1 & 1 & 1 & 1 & 1 \\ 1 & 1 & 1 & 1 & -1 & -1 \\ 1 & 1 & -1 & -1 & 1 & -1 \\ 1 & 1 & -1 & 1 & -1 & 1 \\ 1 & -1 & 1 & -1 & -1 & 1 \\ 1 & -1 & -1 & 1 & 1 & -1 \end{bmatrix},$$

and the only identifiers in which all the digon-contributors are positive are $(13)(25)(46)$, (164523), $(16)(23)(45)$, and (132546) and there are none where they are all negative. Using a computer, we checked the small cases for each edge-monic family, and it is clear that we cannot simply give all digons the same sign. However, the question of how the signed digon structure alone shapes the determinant seems central to Hadamard's Conjecture. The next step is to see if we can determine how digon signs affect the signs of other contributors in a given edge-monic tail-equivalence class. Perhaps we will find there is a special relationship to Hadamard's $4k$ conjecture.

Throughout these sections on the symmetries between classes, we have observed a number of different relationships between contributors. We have in these sections seen both relationships between edge-monic activation classes and contributors within an edge-monic class as well as the construction of fundamental sets. While each of these results has led to progress on Hadamard's Conjecture, we have yet to obtain a concluding result. In many ways these sections each represent a different attempt at solving the conjecture, and the relationships between these different approaches have yet to be fully examined. In future work, we hope that combining the results discussed in each section will allow us to find a formula for the maximum determinant and answer the question regarding the $4k$ conjecture.

REFERENCES

[1] Guido Barba. Intorno al teorema di hadamard sui determinanti a valore massimo. *Giorn. Mat. Battaglini*, 71:70–86, 1933.

[2] Francesco Belardo and Slobodan Simić. On the laplacian coefficients of signed graphs. *Linear Algebra and its Applications*, 475:94–113, 2015.

[3] Richard P. Brent and Judy-anne H. Osborn. On minors of maximal determinant matrices. *Journal of Integer Sequences*, 16(13.4.2):1–30, 2013.

[4] R.L. Brooks, C.A.B Smith, A.H. Stone, and W.T. Rutte. The dissection of rectangels into squares. *Duke Mathematical*, 7:312–340, 1940.

[5] Seth Chaiken. A combinatorial proof of the all minors matrix tree theorem. *SIAM Journal on Algebraic Discrete Methods 3*, 3:319–329, 1982.

[6] G. Chen, V. Liu, E. Robinson, L. J. Rusnak, and K. Wang. A characterization of oriented hypergraphic laplacian and adjacency matrix coefficients. *Linear Algebra and its Applications*, 556:323 – 341, 2018.

[7] V. Chen, A. Rao, L.J. Rusnak, and A. Yang. A characterization of oriented hypergraphic balance via signed weak walks. *Linear Algebra and its Applications*, 485:442–453, 2015.

[8] J. H. E. Cohn. Hadamard matrices and some generalisations. *The American Mathematical Monthly*, 72(5):515–518, 1965.

[9] D. Cvetkovic, M. Doob, and H. Sachs. *Spectra of Graphs: Theory and Applications, 3rd revised and enlarged edition.* Oxford Science Publications. Wiley-VCH, 1998.

[10] Jack Edmonds and Ellis L. Johnson. Matching: A well-solved class of integer linear programs. In *Combinatorial Structures and their Applications (Proc. Calgary Internat., Calgary, Alta., 1969)*, pages 89–92. Gordon and Breach, New York, 1970.

[11] Hartmut Ehlich. Determinantenabschätzungen für binäre matrizen. *Math. Z.*, 83:123–132, 1964.

[12] W. Grilliette, J. Reynes, and L. J. Rusnak. Incidence hypergraphs: Injectivity, uniformity, and matrix-tree theorems. *ArXiv:1910.02305 [math.CO]*, 2019.

[13] Will Grilliette, Deborah Seacrest, and Tyler Seacrest. On blow-ups and injectivity of quivers. *Electronic J. Combinatorics*, 20(2)(#P40), 2013.

[14] J. Hadamard. Résolution d'une question relative aux déterminants. *Bulletin des Sciences Mathématiques.*, 17:240–246, 1893.

[15] F. Harary. On the notion of balance of a signed graph. *Michigan Math. J.*, 2(2):143–146, 1953.

[16] H. Kharaghani and B. Tayfeh-Rezaie. A hadamard matrix of order 428. *J. Combin. Des.*, 13:435–440, 2005.

[17] N. Reff and L.J. Rusnak. An oriented hypergraphic approach to algebraic graph theory. *Linear Algebra and its Applications*, 437(9):2262–2270, 2012.

[18] Nathan Reff. Intersection graphs of oriented hypergraphs and their matrices. *Australas. J. Combin.*, 65:108–123, 2016.

[19] Nathan Reff and Howard Skogman. A connection between Hadamard matrices, oriented hypergraphs and signed graphs. *Linear Algebra Appl.*, 529:115–125, 2017.

[20] L. J. Rusnak, E. Robinson, M. Schmidt, and P. Shroff. Oriented hypergraphic matrix-tree type theorems and bidirected minors via boolean ideals. *J Algebr Comb*, 49(4):461—473, 2019.

[21] L.J. Rusnak. Oriented hypergraphs: Introduction and balance. *Electronic J. Combinatorics*, 20(3)(#P48), 2013.

[22] W. T. Tutte. *Graph theory*, volume 21 of *Encyclopedia of Mathematics and its Applications*. Addison-Wesley Publishing Company Advanced Book Program, Reading, MA, 1984. With a foreword by C. St. J. A. Nash-Williams.

[23] W. Wojtas. On hadamard's inequality for the determinants of order non-divisible by 4. *Colloq. Math*, 12:73–83, 1964.

[24] Thomas Zaslavsky. Orientation of signed graphs. *European J. Combin.*, 12(4):361–375, 1991.